ORKUSTOFNUN
NATIONAL ENERGY AUTHORITY

LEAKAGE FROM SIGALDA RESERVOIR

Snorri Páll Kjaran
Jónas Elíasson

SPK-80/01 November 1980

ORKUSTOFNUN
NATIONAL ENERGY AUTHORITY

GRENSÁSVEGI 9,
108 REYKJAVÍK ICELAND

LEAKAGE FROM SIGALDA RESERVOIR

Snorri Páll Kjaran
Jónas Elíasson

SPK-80/01 November 1980

ORKUSTOFNUN

Dags. 1980-11-25 | Tilv. vor SPK/vp
Dags. | Tilv. yðar

Mr. Rögnvaldur Thorlaksson
Head of Construction
Landsvirkjun
Háaleitisbraut 68
105 Reykjavík

Subject: Leakage from Sigalda Reservoir.

Dear Sir,

In our letter of May 29th 1979 we presented the main results of the Sigalda leakage model calculations. The results have been discussed with Dr. Haefeli of VIRKIR-ELECTROWATT, Mr. D. Deere, Landsvirkjun special consultant and Landsvirkjun representatives. These results indicated considerably higher leakage than earlier anticipated. In our letter of July 6th 1979 some explanations were given as well as recommendations for further investigations in the lava fields south-east of the reservoir (the long path leakage area). The hypothesis was put forward, that the Sigalda Ridge and an oval hill of móberg, 2 km to the southeast, were connected by a ridge of móberg at rather shallow depth below the lava surface. The existance of such an underground ridge of móberg, far less permeable than the lavas, lengthens the long leakage path which again diminishes the gradients and lessens the long path leakage discharge. It was decided to check this hypotheses by drillings. The drillhole data supported the hypothesis of a móberg ridge under the uppermost lava. The model calculations were repeated with new boundary conditions taking this móberg ridge into account. It is our intention in this letter to summarize the results of this investigation. A full report will follow later. The summary is in exhibit 1.

In our letter of July 6th 1979 we pointed out the necessity of drilling piezometer holes along the long leakage path, in order to check the calculations. Two observation piezometer holes were therefore drilled together with the above mentioned drillings. Observations have however been insufficient to verify the calculations. It is therefore important to maintain continuous measurements in one of the piezometers.

8

We hope these calculations are of value to you and remain at your service should you require further clarification.

Jónas Elíasson.

Snorri Páll Kjaran.

LEAKAGE FROM SIGALDA RESERVOIR Exhibit 1.

1 Available data

Our calculations are based on the large amount of data collected during the eight impoundings of the reservoir. The impounding history of the reservoir is shown in figs. 2 and 3. The measurements used are a) water level recordings in piezometer holes and b) flow measurements, at measuring weirs near the dam and discharge measurements in the almost dry Tungnaá River Canyon upstream of the Sigalda waterfall. These measurements are presented in the report "Summary of Impounding Data until November 1977 and Reevaluation of the Hydro-Geological Conditions" (by Messrs. P. Jóhannesson, S. Arnalds, D. Egilson and B. Jónasson, Febr. 1978) and several EWI/Virkir reports. All our calculations are based upon stationary values, that is to say flow and water level values, when the reservoir has been stationary at the same level for a long time compared with the response time of the piezometers. In our further analyses we have plotted the following measurements vs. reservoir level.

A. Flow measurements

1. MW-1 (canal-measuring weir)
2. MW-2 " " "
3. MW-3+MW-4 " " "
4. Increased springflow, i.e. springflow measured in the Tungnaá Canyon minus flow in the canals and initials springflow.

B. Water level measurements for model calibration

1. PZ-15
2. PZ-16
3. PZ-17
4. PZ-18

5. PZ-19
6. PZ-20
7. E - 8
8. TK- 2
9. E -28

C. Water level measurements for model verification

1. SA- 2
2. SA- 3
3. VII
4. TK-12
5. VI
6. V
7. IX
8. PJ-11
9. PJ-12

The location of piezometers and flow measurement sites is shown in figs. 4 and 9. The piezometers mentioned under item B are used to calibrate the model, while the piezometers mentioned under item C are used for verification purposes in order to check the model calculations.

2. Geological factors

A geological map of the model area is shown in fig. 1, which also indicates the probable extension of the Sigalda móberg at shallow depth. The southern banks of the reservoir are made of the socalled TH_h-lava, overlaying the Th_f-lava which covers most of the reservoir bottom. The Th_h-Th_f contact is at approx. 478 m a.s.l. and is rather scoriaceous, especially the lower part of the Th_h-lava. In the vicinity of the dam Th_c is overlain by the Th_f-lava, and the Th_f-Th_c contact has shown itself to be an effective aquifer.

The reservoir area is a former lakebasin, with maximum water level at app. 500 m a.s.l. Clay deposits of varying thickness have therefore

covered the lavas, and clay has been deposited in the Th_h-Th_f contact, obviously because of leakage from the lake. A narrow strip along the Th_h-front is therefore tighter than the contact elsewhere, except perhaps in the Hnubbafossar area where the lavas are heavily eroded. Another erosion feature, the Sigalda canyon, later drained the old lake, and created numerous springs. There is no doubt that the disappearance of the old lake has caused a regional lowering of the groundwater table. This has the immediate effect, now the dam is built, and the lake restored without raising the groundwater table to its old level, that the clay deposits are subjected to greater differential pressures than before. This causes piping in the clay seal into cracks and cavities in the lava and the formation of swallow holes that increase in number when the water level is raised. Another effect of the emptying of the former reservoir lake has been surface water erosion in the reservoir bottom, particularly in the riverbed and on steep slopes like Th_h-lava front, creating conditions for infiltration and swallow holes formation.

3. Canal flow data

The flow in MW-1, the old diversion canal, is shown in fig. 5 vs. reservoir level. The relationship is seen to be linear. This flow comes from the Th_f-lava.

The flow in MW-2 is shown in fig. 6 vs. reservoir level. Before the 6th impounding there seems to be some square component in the flow, curving the data points to the right. At the 6th impounding the relationship is clearly linear again. Before the 6th impounding MW-2 had inflow from both the Th_f-lava and the Th_h-Th_f contact scoria. After the 5th impounding the inflow from the Th_h-Th_f contact scoria was diverted into MW-3 and MW-4 and thus just the Th_f-lava contributed to the flow in MW-2.

The flow in MW-3 and MW-4 is shown in fig. 7. Clearly both a linear and a square component are present in the flow, and field observations indicate clearly, that both of the canals have inflow from the Th_f-lava and the Th_h-Th_f contact scoria.

It can therefore be concluded that the canals have a linear flow component from the Th_f-Th_c lava and a square flow component from the Th_h-Th_f contact scoria. Clearly the sealing work performed after the third impounding resulted in insignificant reduction of the canal flow.

4. Springflow data

Increased springflow is shown in fig. 8. It can be shown that the increased springflow varies with the square of the reservoir water level height above 478 m a.s.l. This result is in agreement with the canal analysis indicating that the square component originates from the Th_h-Th_f contact scoria. According to the flow measurements the sealing work has significantly reduced this flow. This result is incompatible with the piezometer level data as discussed in ch. 8.

5. Piezometer level data

Location map for the pizometers used in the analysis is shown in fig. 9. Stationary values for the piezometer level vs. reservoir level is shown in figs. 10-18. The piezometer level is the potential head of the Th_h, Th_f and Th_c-lavas. The relationship between the reservoir level and the piezometers seems to include the same square and linear components found in the relationship between the reservoir level and the flow measurements. There seems to be some evidence that the sealing work has actually reduced the rise in the piezometer levels, but this indication is considerably less than might be expected from the increased springflow measurements, see fig. 8.

In the following we write the piezometer level of the form:

$$h-h_o = k_2(H-478)^2+k_1(H-476.5)$$

The zero level, h_o, is shown in fig. 9 and the constants k_2 and k_1 are shown in figs. 45-48.

6. Data analysis

To establish a relationship between the flow data and the piezometer level data that is compatible with the geological factors, it is necessary to separate and explain separately the linear and square components. Although the permeability is great in the area the gradients are very small; thus a turbulent flow model explaining the square component in the piezometer level is not possible. Fig. 19 shows stationary values for the piezometer level in E-28 vs. flow in the canyon. The relationship is seen to be linear in the form

$$Q = 2.196\ h - 1046.829$$

with a correlation coefficient of 0.995. The global groundwaterflow is therefore likely to follow Darcy's law, and turbulent flow model is thus not possible. It can be seen from the above equation that one meters difference in piezometer level gives 2.2 m^3/s difference in flow values. Our explanation is that the inflow from the reservoir into the Th_h-Th_f contact scoria is mostly due to swallow holes formed by the differential pressure on the reservoir clay. The water level in the piezometers is proportional to nQ, where n is the number of swallow holes and Q is the inflow into each one. Q is again proportional to H-h, where H is the reservoir height and h the piezometer height above the Th_h-Th_f contact level. The simplest relationship for n is $n \sim H$. We therefore have $h \sim H(H-h)$, that is:

$$h = \frac{\delta}{1+\delta H} \cdot H^2,$$

which can be approximated by $h = k_2 \cdot H^2$. The formulas of the straight lines and parabolas fitted to the measured flow values and shown in figs. 5-8 are listed in table 1. The respective coefficients for the piezometer parabolas are shown in figure 9 and figures 45 to 48. The reference level 478 m a.s.l., used in the formula, is the level of the Th_h-Th_f contact scoria, see ch. 2. The reference level 476.5 m a.s.l. is the lake level when the groundwater gradients from the reservoir to the aquifer are reversed.

TABLE 1

Measured outflow in m^3/s

BEFORE SEALING WORK

Initial springflow	:	4.5
Increased springflow	:	$0.04869(H-478)^2$
MW-2+MW-4	:	$0.01044(H-478)^2+0.1639(H-476.5)$
MW-2	:	$0.12166(H-476.5)$
MW-1	:	$0.0845(H-476.5)$
Total square	:	$0.05913(H-478)^2$
Total linear	:	$0.3701(H-476.5)$

AFTER SEALING WORK

Initial springflow	:	4.5
Increased springflow	:	$0.02486(H-478)^2$
MW-3+MW-4	:	$0.01044(H-478)^2+0.1639(H-476.5)$
MW-2	:	$0.12166(H-476.5)$
MW-1	:	$0.0845(H-476.5)$
Total square	:	$0.0353(H-478)^2$
Total linear	:	$0.3701(H-476.5)$

H: reservoir water level in m a.s.l.

7. Numerical modeling

It has been seen that the inflow/outflow is written in the form

$$Q-Q_o = C_2(H-478)^2+C_1(H-476.5)$$

and the pizometerlevel in the form

$$h-h_o = k_2(H-478)^2+k_1(H-476.5).$$

The only mathematical solution to this problem is that k_1 and k_2 correspond to C_1 and C_2 respectively. We have therefore determined the necessary distribution of the inflow/outflow from the area to match the linear and square components in the piezometer level. For this purpose Laplace's equation is solved with the appropriate boundary conditions in a finite element grid numerical computer model. For the sake of simplicity the permeability of the area is assumed constant. The Laplace equation is solved twice, once for the linear and square flow components respectively. The finite element grid is shown in fig. 20 and 21 with the appropriate boundary conditions. The boundary condition in Sigalda Canyon is the so called spillway boundary condition given by:

$$T\frac{\delta h}{\delta n} = \alpha h$$

where T is the transmissivity, $\frac{\delta h}{\delta n}$ the gradient, h the piezometric level and α a proportionality constant. Fig. 19 confirms this boundary condition. In order to establish the remaining boundary conditions the boundary piezometers are analysed. The time variations of the boundary piezometers for eight impoundings of the reservoir are shown in figs. 22-33. Comparing these figures with the impounding history, figs. 2 and 3, reveal the following:

a) The boundary piezometers in the west, II, III and IV are seen to depend on the reservoir level. The boundary conditions in the two lava passes in the west are thus considered two unknown boundary outflow values.

b) The two boundary piezometers in the south, TH-10, TH-11, are seen to be independent of the reservoir level. The piezometric level in TH-10 is more dependent on natural groundwater inflow than reservoir level. The boundary condition in the southern lavapass is thus considered a no flow boundary. c) The boundary condition at the lake is considered

an unknown inflow boundary. The móberg formations are considered to be watertight.

From the boundary piezometric level data the constants k_1 and k_2 for II, III and IV are determined and given in the following table

BOUNDARY PIEZOMETERS

Piezometers / Piezometer constants	II	III	IV
k_1	0	$3.39 \cdot 10^{-2}$	$1.53 \cdot 10^{-2}$
k_2	$1.00 \cdot 10^{-2}$	$5.48 \cdot 10^{-3}$	$5.42 \cdot 10^{-3}$

If there is a 10 m rize in reservoir level the piezometric level rises 10 k_1 meters according to the linear flow and 100 k_2 meters according to the square flow. Estimation of the constants from the available boundary piezometric data was very difficult owing to paucity of measurements and lack of information as to the natural flow variations. In the following we therefore use the constants between limits defined by

$$0 \leq k \leq \beta \cdot k_{table}$$

where β is some constant.

In the case of the linear flow component we take the reservoir inflow to consist of two unknown inflow values, see fig. 45 and 46. According to former geological investigations the Th_f-lava was not found in boundary piezometer II. Therefore it is assumed that the extension of the Sigalda móberg closes this lavapass off completely. The outflow values in the two passes in the west therefore consist of two unknown outflow values for the square flow, but only one unknown for the linear-flow. We therefore have three (four) unknown flow values. These unknown flow values are determined by matching the measured and calculated piezometric levels in such a way that the following norm is minimized.

$$L = \Sigma (k_1^{measured} - k_1^{calculated})^2$$

where L is the norm to be minimized, the summation is taken over the number of boreholes and $k_1^{measured}$ and $k_1^{calculated}$ is the linear constant from measurements and calculations respectively.

The minimum value of L is known as the residual norm. The unknown boundary outflow parameter, α, in the Sigalda Canyon is now determined by minimizing the residual norm. The result is now shown in figs. 34, 40, 41, 45 and 46. As mentioned above the k values for the boundary piezometers II, II and IV are very uncertain. The sensitivity of the results is now investigated with respect to the parameter β defined above. The result is shown in fig. 35, which shows the residual norm increasing rapidly for β greater than one.
We then select the most probable β interval to be $0 \leq \beta \leq 1$. Fig. 36 shows catchment loss divided by measured loss against β; since β lies between zero and one we have

$$1.7 \leq {}^{\text{Catchment loss}}/_{\text{Measured loss}} \leq 1.8$$

Where catchment loss is the outflow in the lava passes in the west, and measured loss is the measured flow in Sigalda Canyon minus the initial springflow and the flow in MW-1 and MW-2.
The same procedure is now repeated for the square flow component. The minimum α-value is shown in fig. 37 and the piezometric level in figs. 42, 43, 47 and 48. The β interval is determined from fig. 38 to be $0 \leq \beta \leq 1$. Fig. 39 then gives for the catchment square flow loss.

$$0.30 \leq {}^{\text{Catchment loss}}/_{\text{Measured loss}} \leq 0.50$$

The result for the combined effect of linear flow and square flow components at lake level 493 m a.s.l. is shown in figs. 44 and 49.

The flow under the dam is not included in the calculations, but taken to correspond to the flow in MW-1 and MW-2.

In order to check the results the water level measurements mentioned in ch. 1C are used for model verification. The comparison between measured and caluculated piezometric level is shown in figs. 50-56.

These water level measurements were not used for model calibration but for verification of the model. The figures show good correlation between the two sets.

8. Results

The reservoir inflow can be separated into a linear component and a square component. The linear component is believed to be flow in the Th_f-lava at the dam and leakage in the Th_h-Th_f contact scoria at Hnubba-fossar.

Heavy drainage of groundwater towards the canyon keeps the groundwater level low in the lavas while the reservoir level rises thus causing increased differential pressure on the clay deposits on the submerged lava fronts. The square component is most likely swallow hole leakage in the Th_h-lava, when the reservoir clay succumbs to differential water pressure. Bearing this in mind the main conclusion to be drawn from the calculations are:

1) The sealing work in 1977, aimed at closing the square component inflow, did not succeed as expected. This can be seen from fig. 57. Here we also have the greatest discrepancy between the model and the flow measurements. According to the model the sealing work would have decreased the square component outflow by about 10%, but springflow measured in the Tungnaá River Canyon indicates a decrease of about 50%. Since the model is based on the piezometric measurements, there is a discrepancy in the relationship between the piezometric measurements and the above mentioned reduction of the springflow. It can also be seen from fig. 8 that early summer impoundings always give more increased springflow than late summer impoundings. In our opinion the reason for this discrepancy is the seasonal variation in the undisturbed natural groundwater level.

   During early summer impoundings the natural groundwater level is higher than during autumn impoundings. Different natural groundwater levels cause different springflow, which is estimated to be a constant equal to 4.5 m^3/sec; although it is of cause higher when natural

groundwater level is high and lower when natural groundwater level is low. The difference between the increased springflow measurements in third and fourth impounding at reservoir level 490 is 3 m^3/sec, (fig. 8). According to fig. 19 this corresponds to a difference in piezometer level in E-28 of 1.4 m. The actual difference in natural groundwater levels between impoundings 3 and 4 may very well have been in the region of one meter.

It is therefore not possible to estimate the effect of sealing work by comparing early summer and autumn flow measurements or even by comparing different years, without knowing the undisturbed natural groundwater level. It should also be pointed out that the square component inflow of the area now covered by the sealing carpet was about one order of magnitude larger than the rest of the inflow (see fig. 47). Therefore the location of the sealing carpet was correctly chosen.

2) The model predicts leakage figures. The following notations have been used for the different leakage values.

Measured loss: Measured flow in Sigalda Canyon. Fig. 58.

Catchment loss: Calculated flow out of the catchment area through the two lava passes in the southwest. Fig. 59.

Total loss: Sum of the measured loss and the catchment loss. Fig. 60.

The model predicts significant loss figures, as shown in fig. 60, which gives both the total loss and the measured loss. It can be seen that the measured loss is about 2/3 of the total loss, and the catchment loss is about 1/3 of the total loss. The loss figures are given between two limits according to the above mentioned limits in the calculations. The catchment loss is greatly influenced by the behaviour of the piezometric level in the southern part of the area, where information is very scarce. SA-2 and SA-3 were drilled in order to improve the situation, but owing to the paucity of measurements they have not been as useful as expected. It is therefore very important to maintain continuous registration of the water level in either SA-2 or SA-3 in order to be able to check the calculations better.

3) The model determines the regional permeability in

the area to be of the order of 40-60 cm/sec. This is in fair agreement with the previously determined permeabilities.

4) The optimum energy reservoir level vs. reservoir inflow is calculated from the model results and given in fig. 61. Three curves are shown in fig. 61. The first gives the optimum energy reservoir level if the leakage consisted only of the measured loss, while the other two give the limits of optimum energy reservoir level for total leakage figures. The limits correspond to the above defined limits for flow values. The calculations are based upon constant efficiency and take only the power output from Sigalda into account. Calculations are now in progress which will take Hrauneyjafoss and Búrfell into consideration with the assumption that the catchment loss is irretrievable for power generation at Hrauneyjafoss and Búrfell.

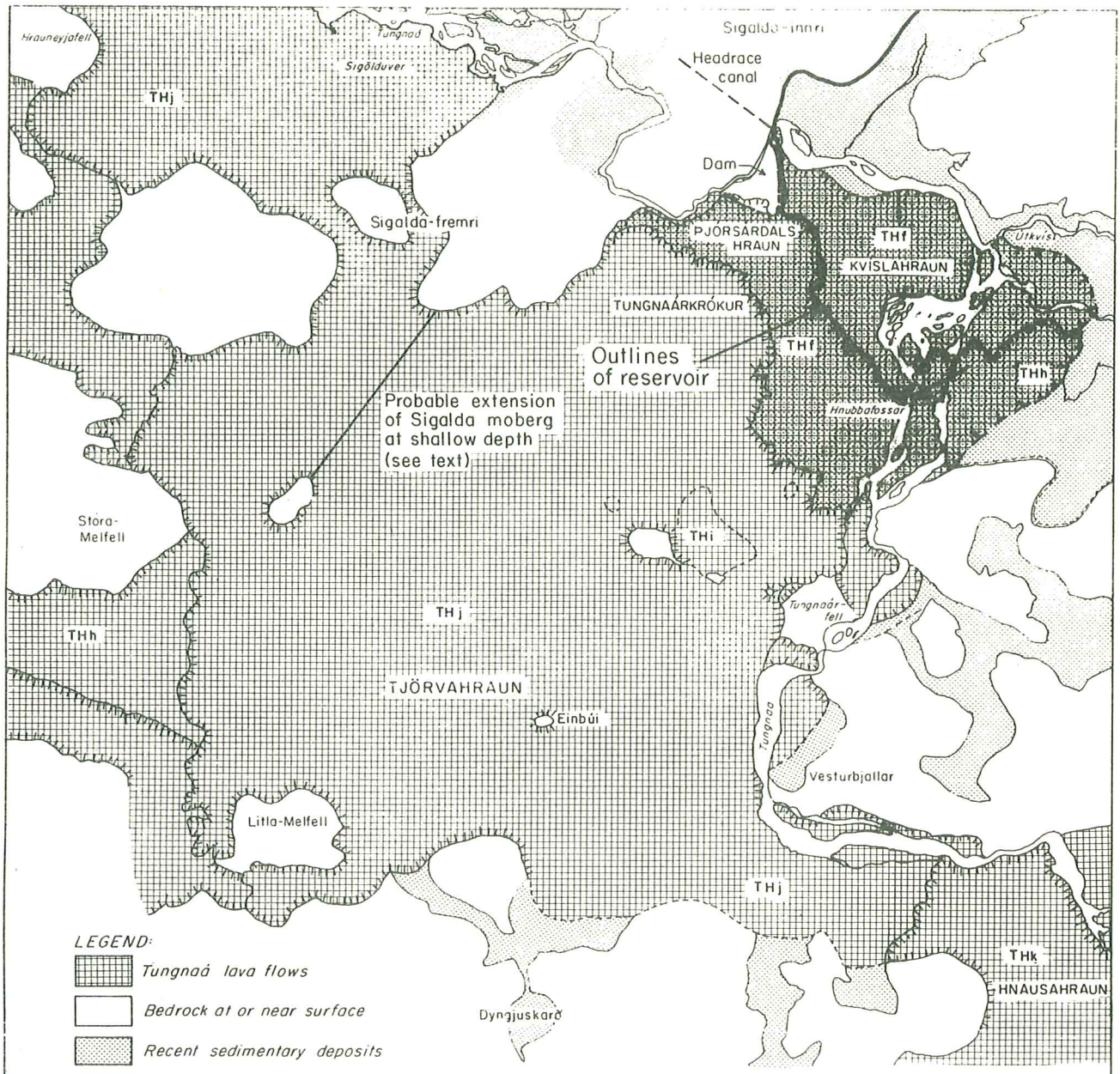

SIGALDA
Geological map

Fig. 1

'80.09.01. SPK/ÓD B-332 F-19952

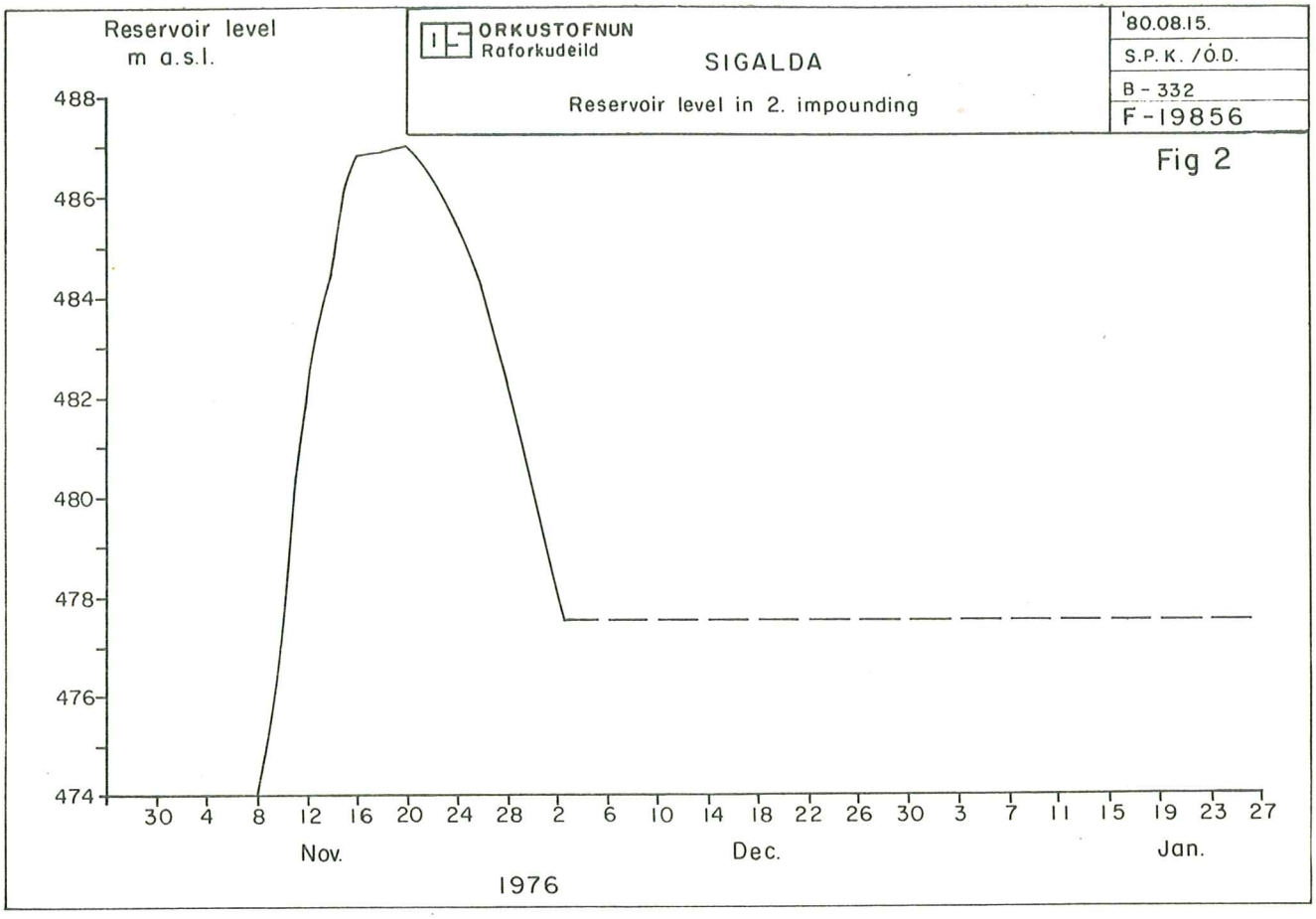
Reservoir level
m a.s.l.
ORKUSTOFNUN
Raforkudeild
SIGALDA
Reservoir level in 2. impounding
'80.08.15.
S.P.K. /Ó.D.
B - 332
F - 19856
Fig 2
488
486
484
482
480
478
476
474
30 4 8 12 16 20 24 28 2 6 10 14 18 22 26 30 3 7 11 15 19 23 27
Nov.
Dec.
Jan.
1976

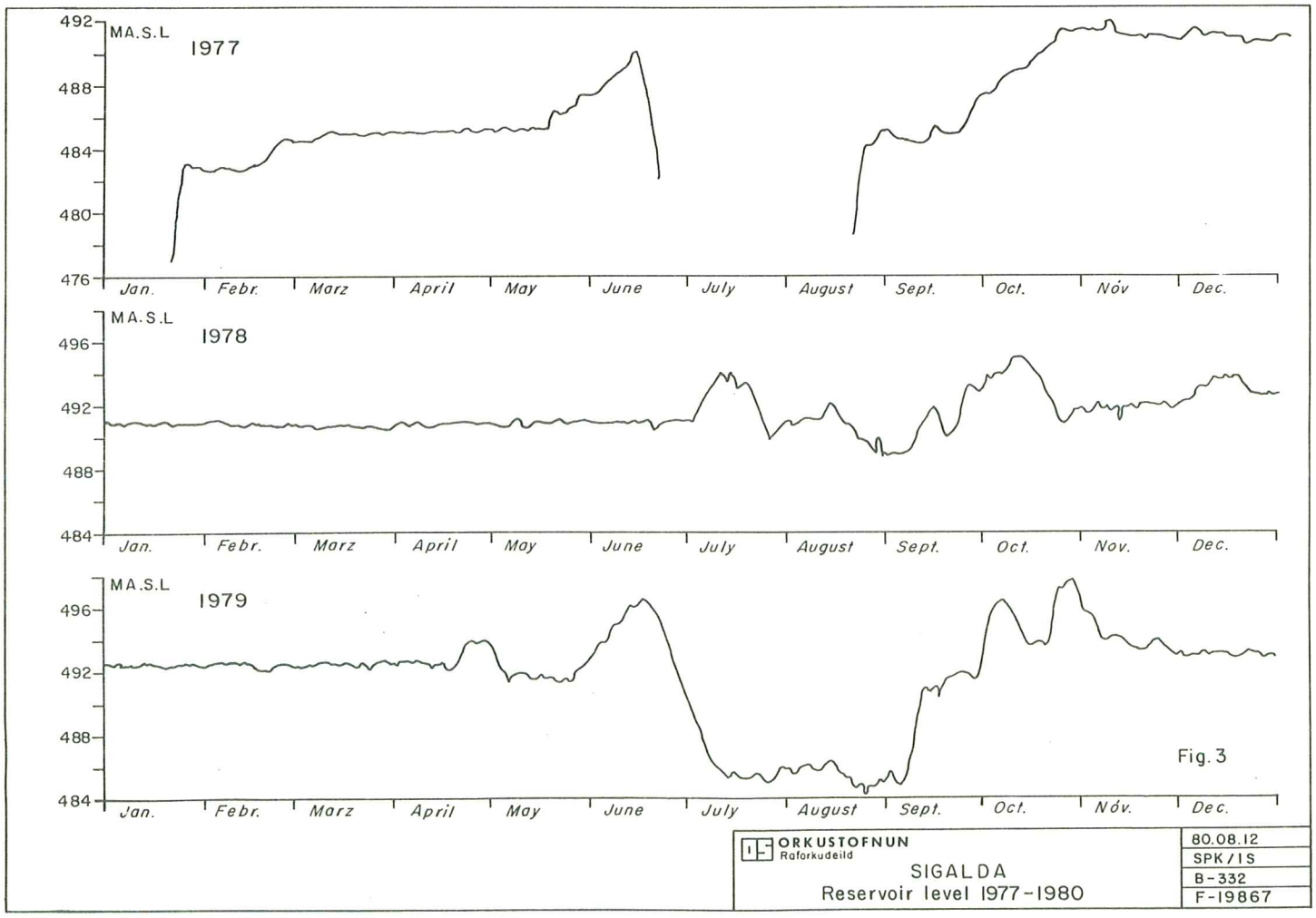
MA.S.L
1977
492
488
484
480
476
Jan. Febr. Marz April May June July August Sept. Oct. Nóv Dec.
MA.S.L
1978
496
492
488
484
Jan. Febr. Marz April May June July August Sept. Oct. Nov. Dec.
MA.S.L
1979
496
492
488
484
Jan. Febr. Marz April May June July August Sept. Oct. Nóv. Dec.
Fig. 3
ORKUSTOFNUN
Raforkudeild
SIGALDA
Reservoir level 1977-1980
80.08.12
SPK/IS
B-332
F-19867

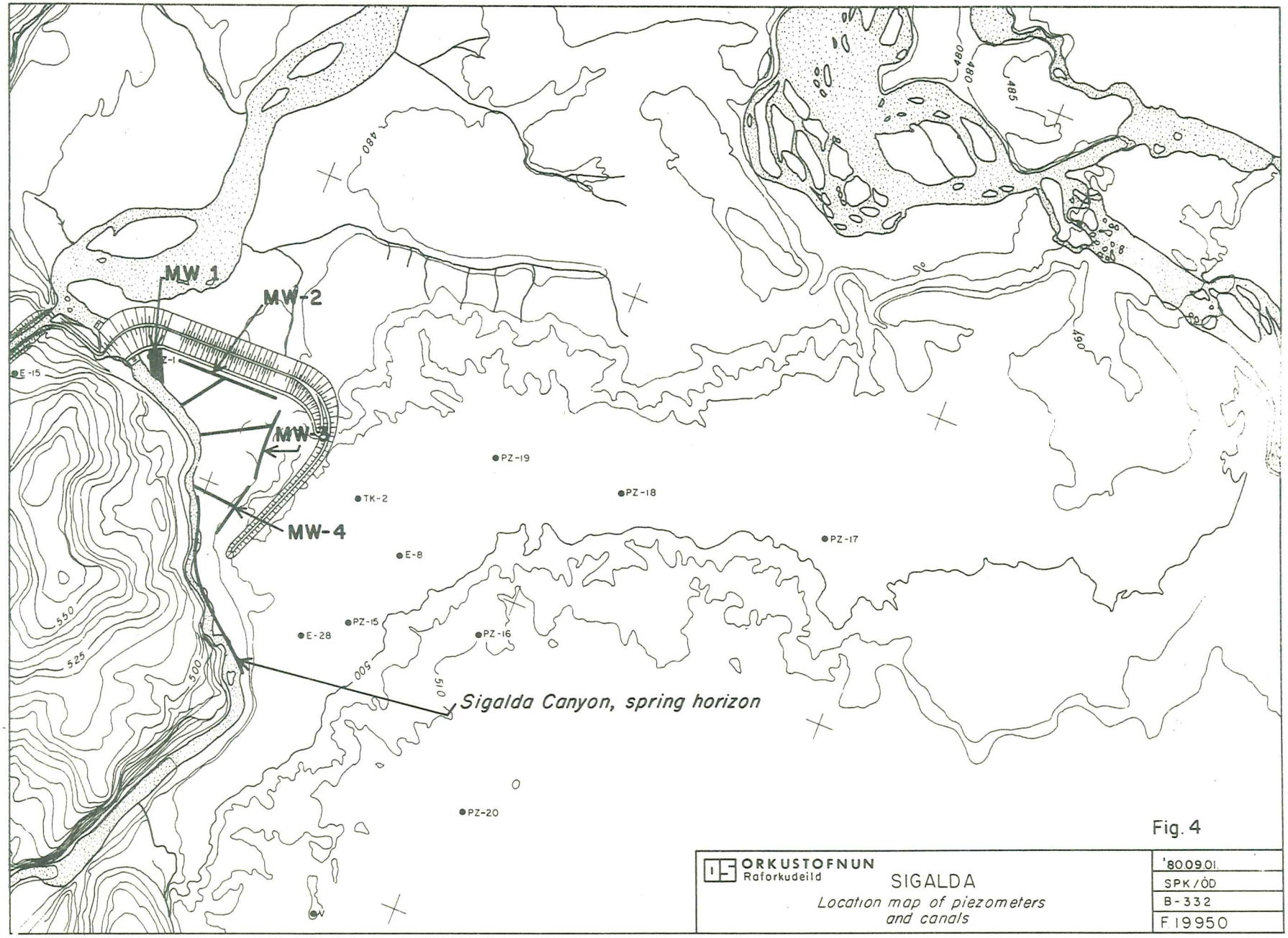

Fig. 4

ORKUSTOFNUN
Raforkudeild

SIGALDA

Location map of piezometers and canals

'80 09 01
SPK/ÓD
B-332
F 19950

ORKUSTOFNUN Raforkudeild

SIGALDA

MW-1 *Discharge vs. Reservoir level*

1979 04 26
D E /Ó D
B-332
F. 18389

Fig. 5

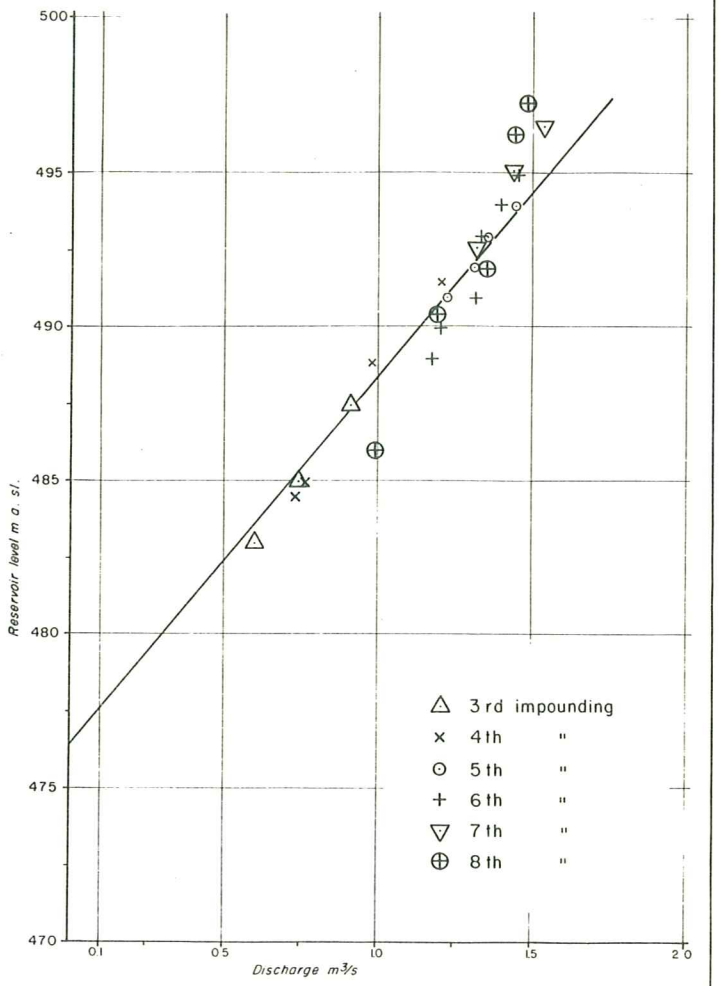

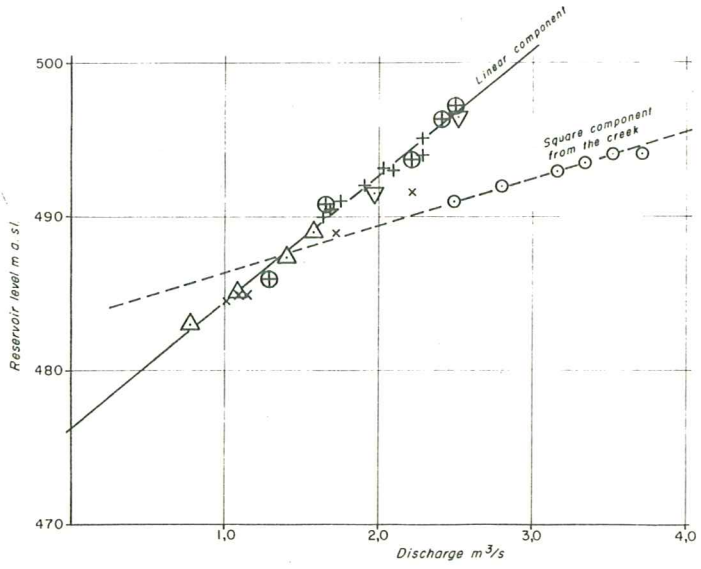

△ 3rd impounding
× 4th "
⊙ 5th "
\+ 6th "
▽ 7th "
⊕ 8th "

Fig. 6

ORKUSTOFNUN Raforkudeild

SIGALDA

MW-2 *Discharge vs Reservoir level.*

1979 04 26
D E /Ó D
B-332
F. 18391

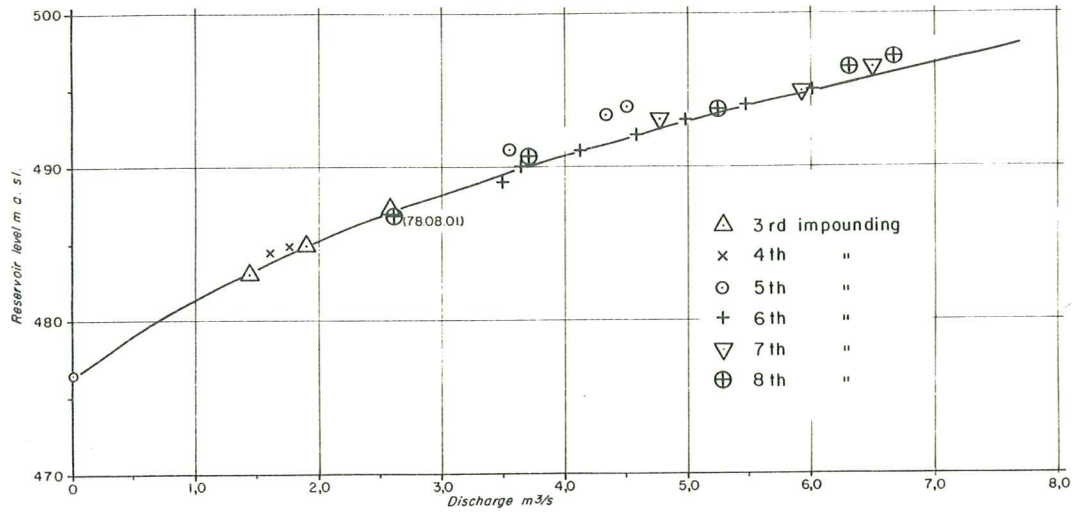

Fig. 7

ORKUSTOFNUN Raforkudeild	SIGALDA	1979 04 26
	MW-3 *and* MW-4 *vs. Reservoir level*	D.E./Ó.D.
		B-332
		F.18390

ORKUSTOFNUN Raforkudeild	SIGALDA	1979 04 26
	Increased springflow vs. Reservoir level	D.E/ÓD
		B-332
		F.18387

Fig. 8

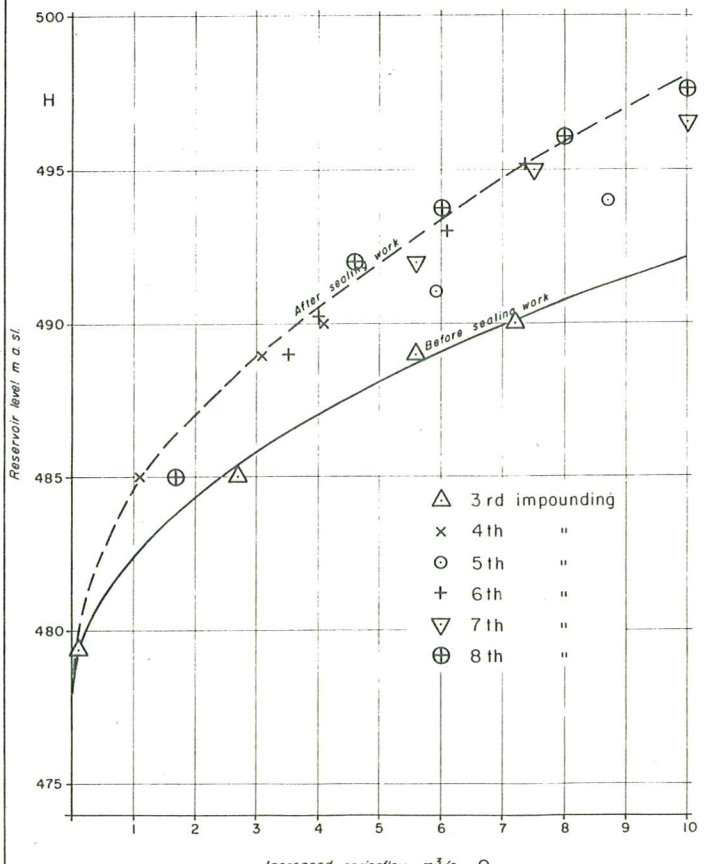

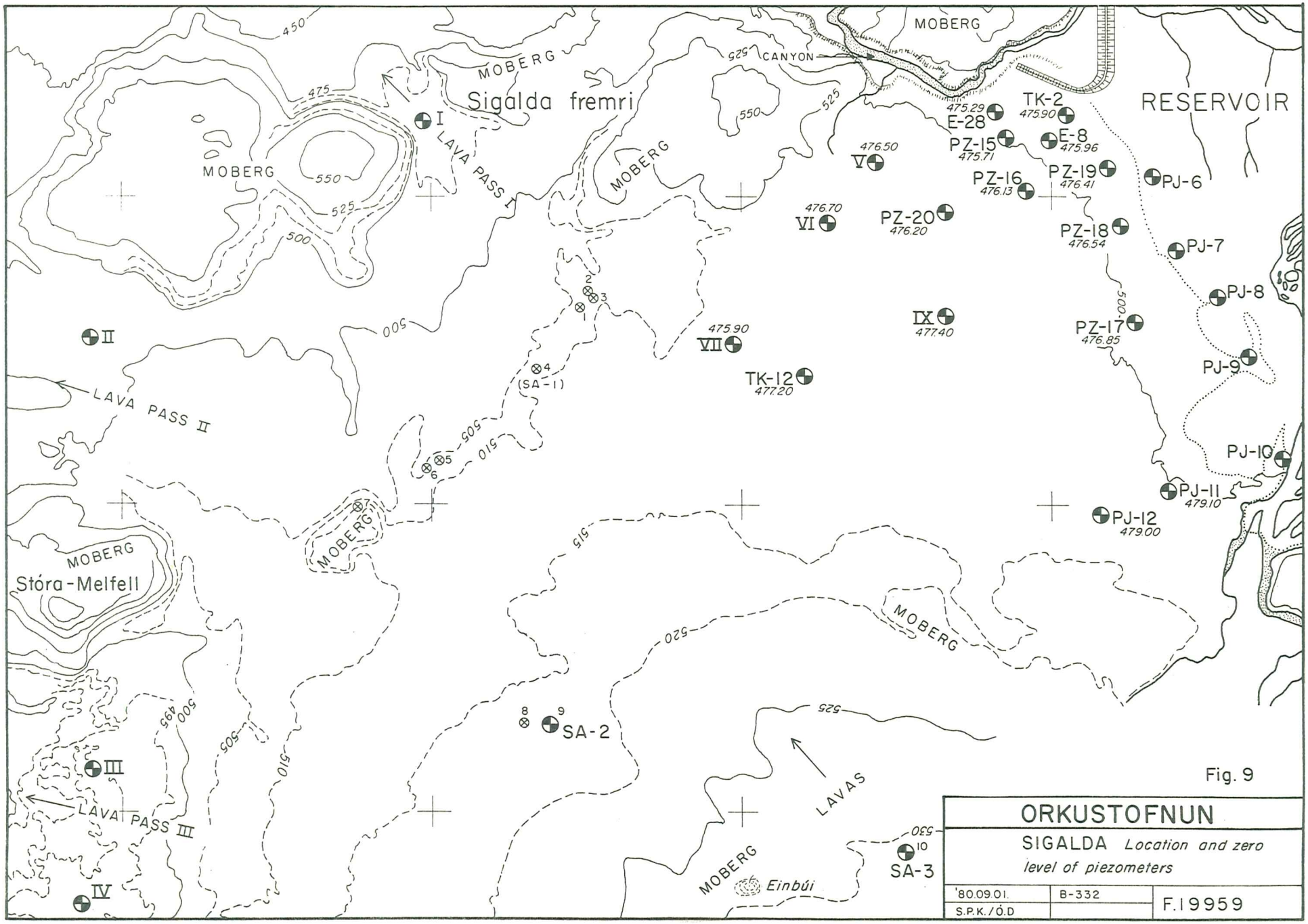

Fig. 9

ORKUSTOFNUN		
SIGALDA *Location and zero level of piezometers*		
'80.09.01.	B-332	F.19959
S.P.K./Ó.D		

ORKUSTOFNUN Raforkudeild

SIGALDA

PZ-16 VS. RESERVOIR LEVEL

1979 04 25 | DE/Gyða | B-332 | F. 18386

Fig. 10

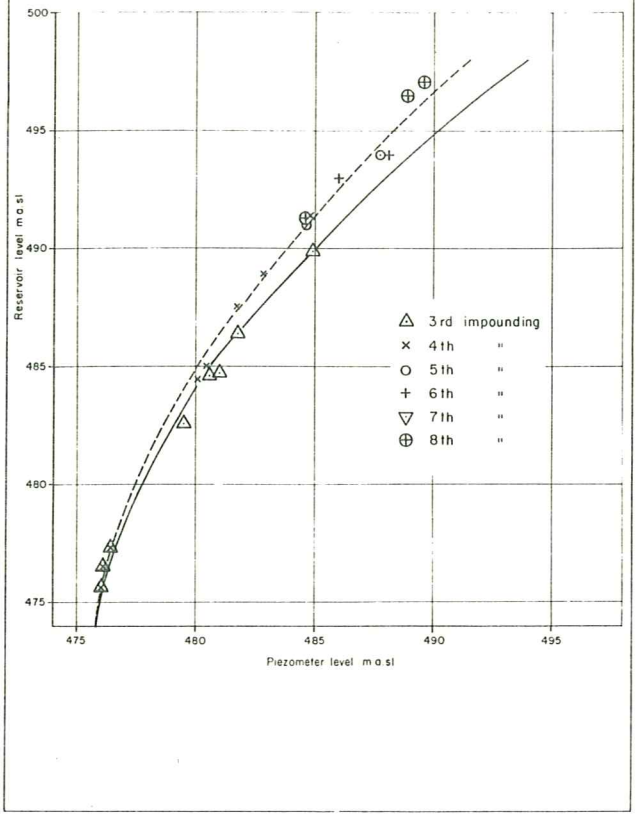

ORKUSTOFNUN Raforkudeild

SIGALDA

TK-2 V.S. RESERVOIR LEVEL

1979 04 25 | DE/Gyða | B-332 | F-18385

Fig. 11

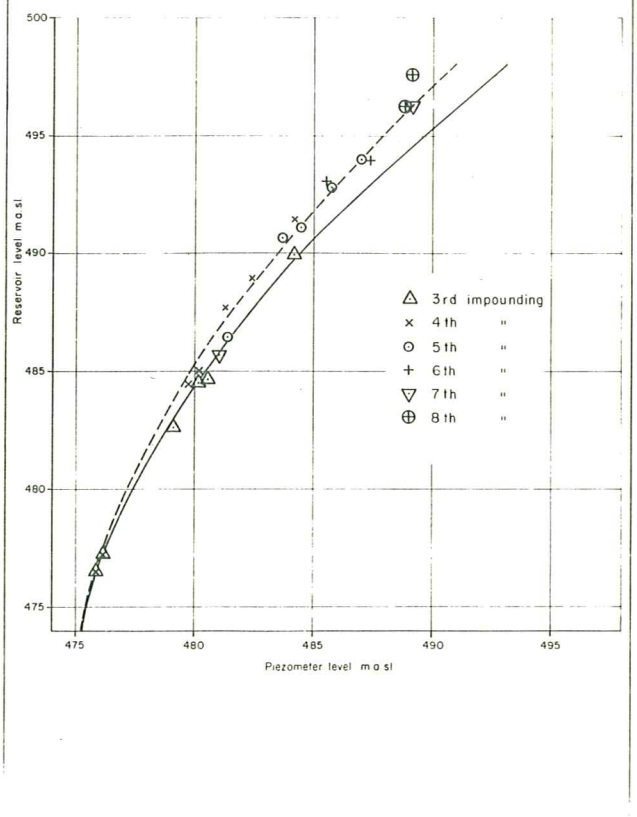

ORKUSTOFNUN Raforkudeild

SIGALDA

E-28 VS. RESERVOIR LEVEL

1979 04 25 | DE/Gyða | B-332 | F-18384

Fig. 12

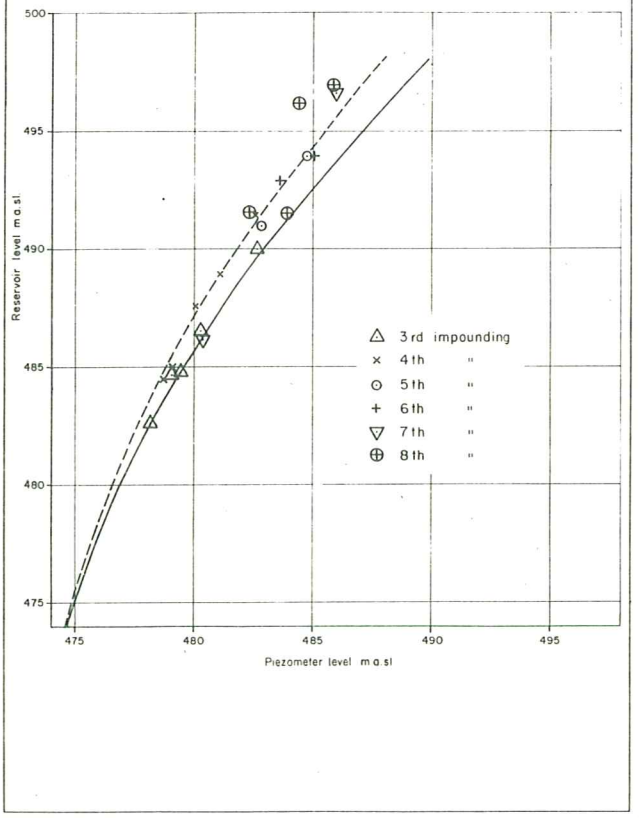

ORKUSTOFNUN Raforkudeild

SIGALDA

E-8 VS. RESERVOIR LEVEL

1979 04 25 | DE/Gyða | B-332 | F-18383

Fig. 13

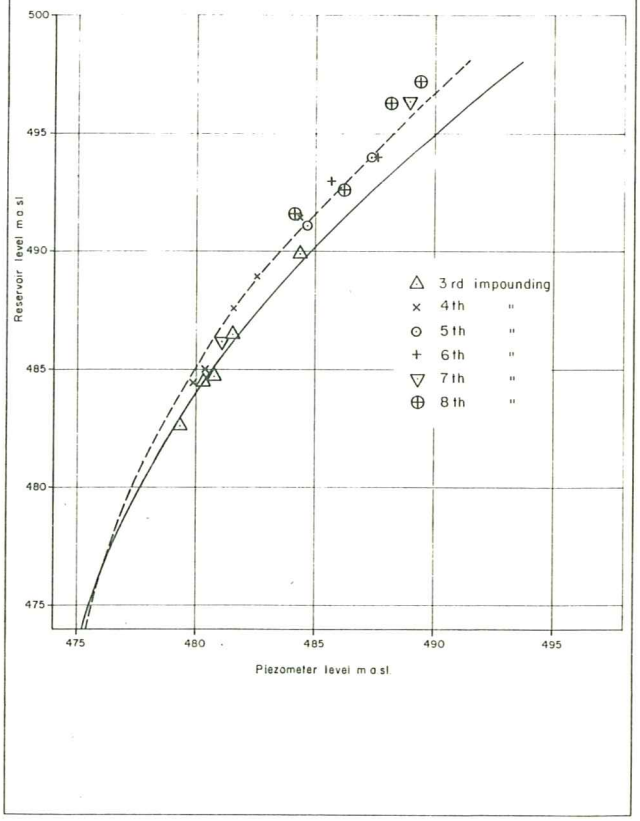

ORKUSTOFNUN Hafarkudeild

SIGALDA

PZ-17 VS RESERVOIR LEVEL

1979 04 25
DE/Gyða
B-332
F-18382

Fig. 14

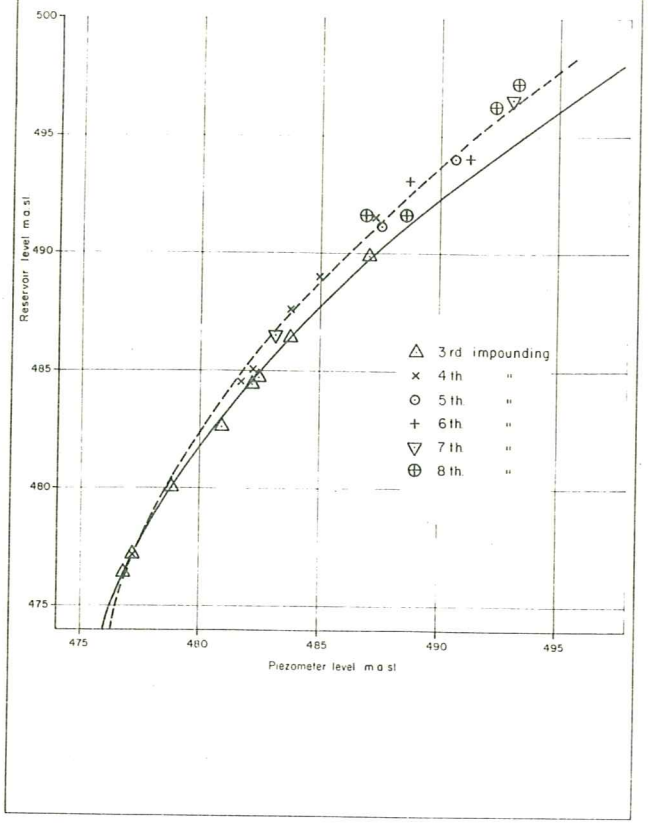

ORKUSTOFNUN Hafarkudeild

SIGALDA

PZ-20 VS RESERVOIR LEVEL

1979 04 25
DE/Gyða
B-332
F-18381

Fig. 15

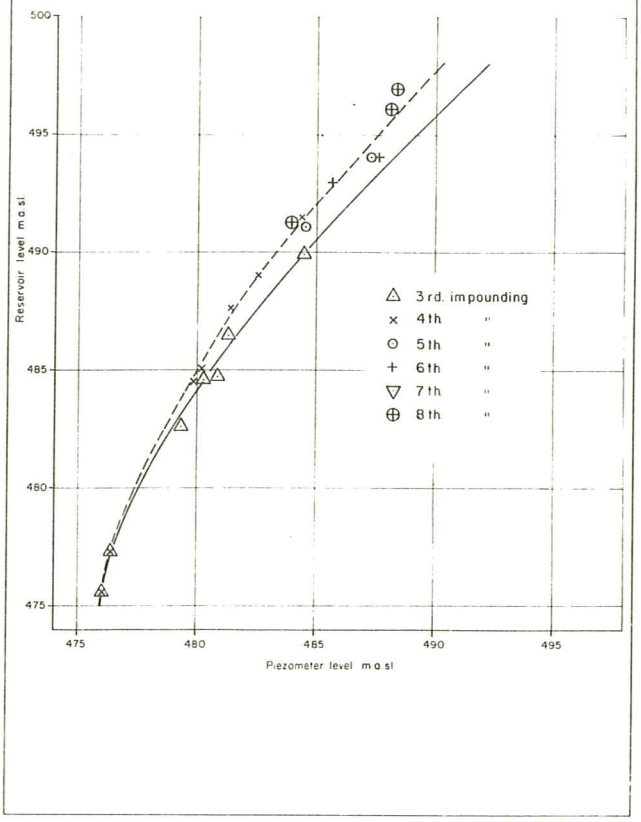

ORKUSTOFNUN Hafarkudeild

SIGALDA

PZ-19 VS RESERVOIR LEVEL

1979 04 25
DE/Gyða
B-332
F-18380

Fig. 16

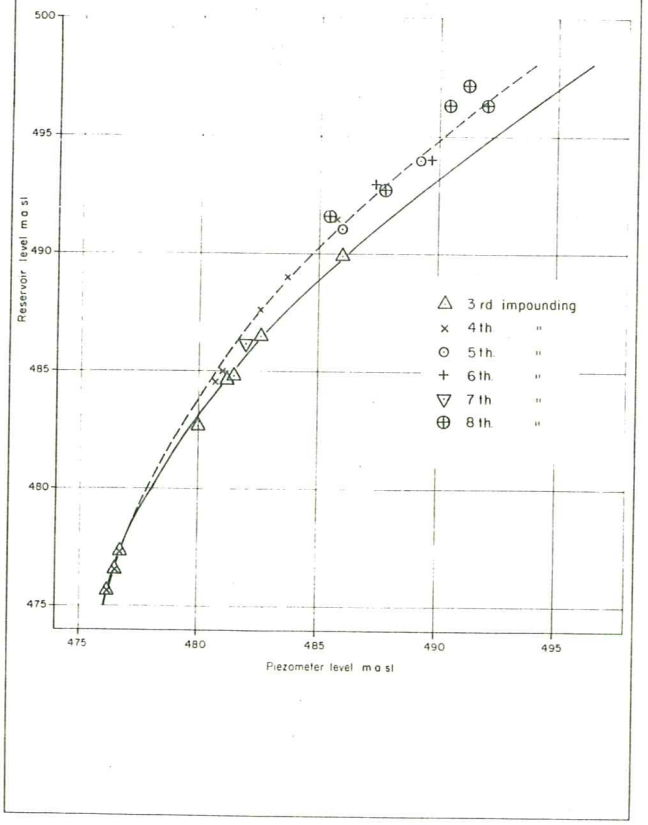

ORKUSTOFNUN Hafarkudeild

SIGALDA

PZ-18 VS RESERVOIR LEVEL

1979 04 25
DE/Gyða
B-332
F-18379

Fig. 17

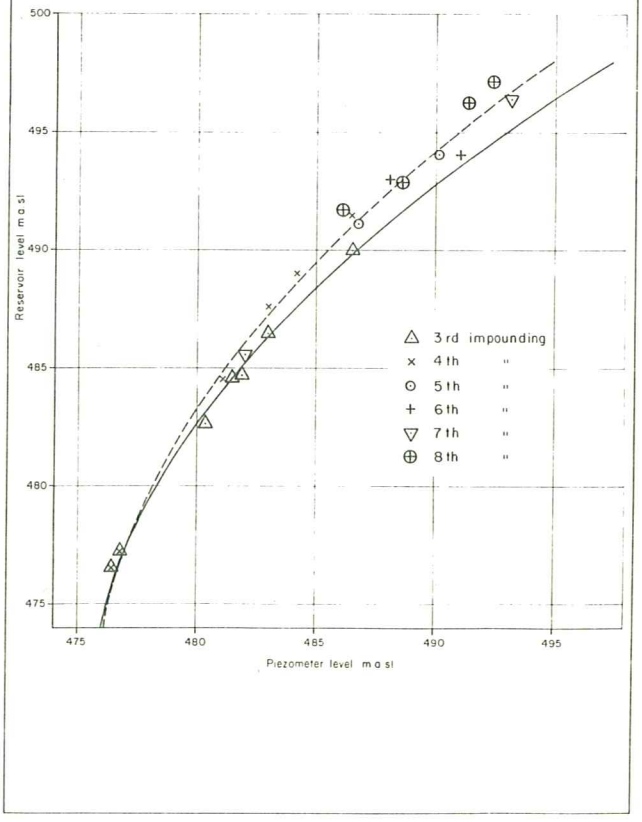

ORKUSTOFNUN Raforkudeild

SIGALDA

PZ–15 VS. RESERVOIR LEVEL

1979 04.25.
DE/Gyða
B-332
F-18376

Fig. 18

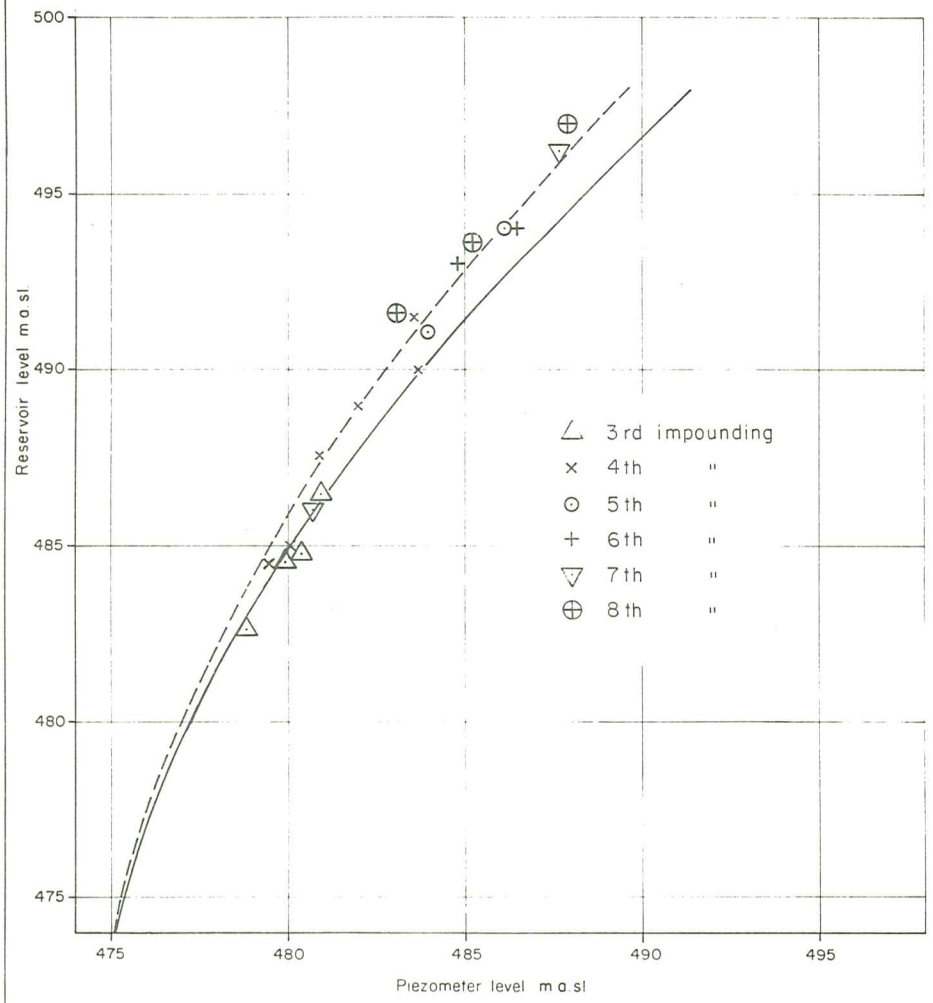

ORKUSTOFNUN Raforkudeild

SIGALDA

Flow in Canyon vs. piezometer level in E-28

'80.09.01.
SPK/ÓD
B-332
F.19948

Fig. 19

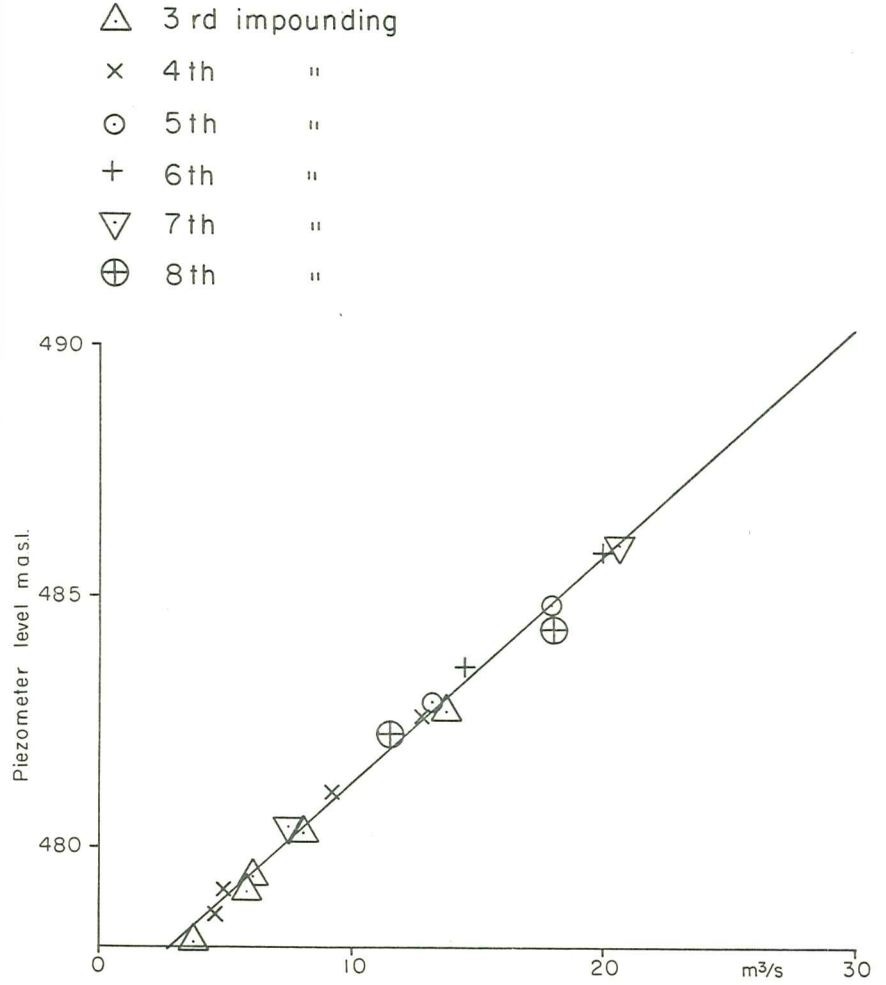

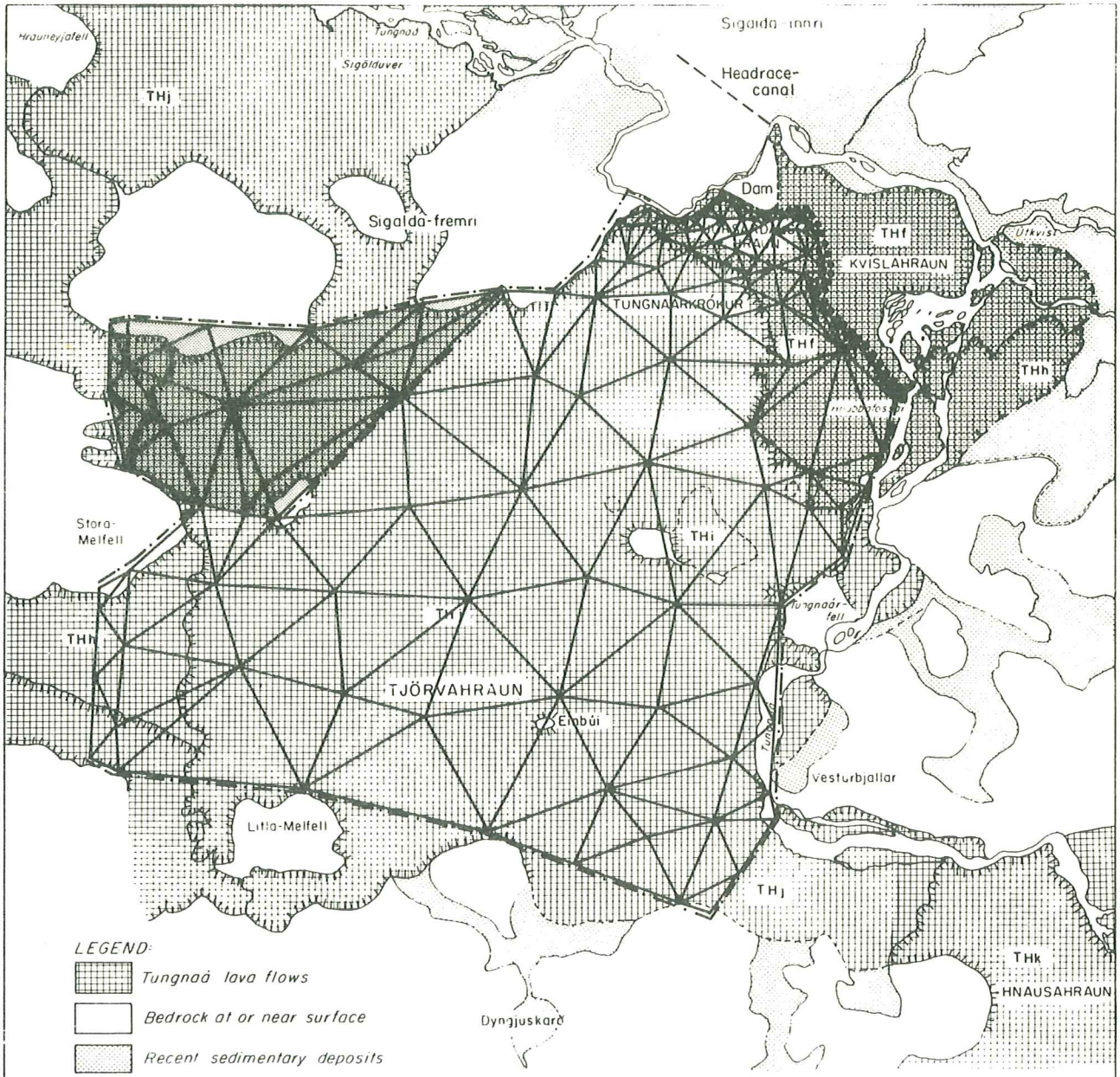

SIGALDA

Triangular mesh

Fig. 20

'80.09C SPK/ÓÐ B-332 F.19958

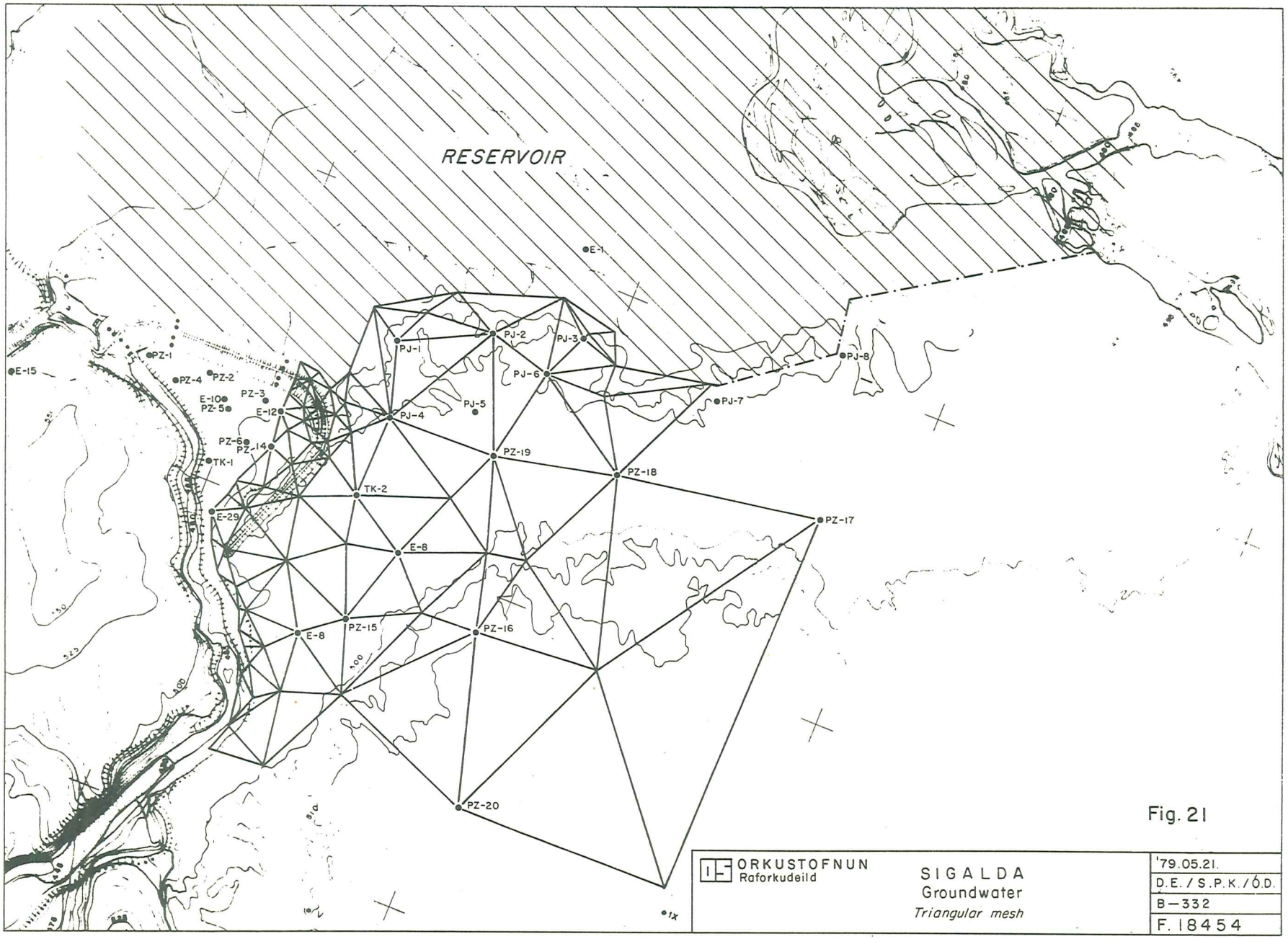

Fig. 21

ORKUSTOFNUN Raforkudeild	SIGALDA Groundwater *Triangular mesh*	'79.05.21. D.E. / S.P.K. / Ó.D. B—332 F. 18454

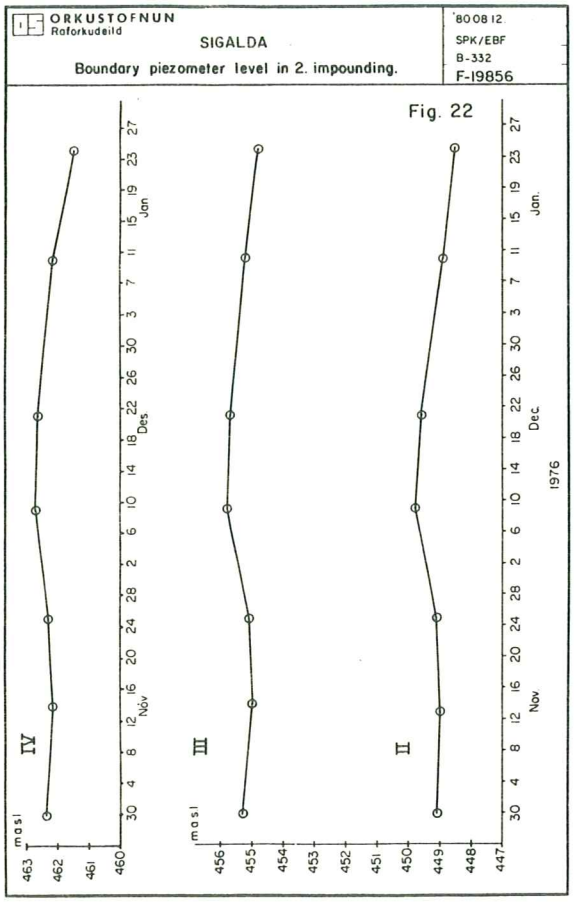
ORKUSTOFNUN
Raforkudeild
SIGALDA
Boundary piezometer level in 2. impounding.
'80 08 12
SPK/EBF
B-332
F-19856
Fig. 22
IV
III
II
m a s l
Nov
Des
Jan
Dec
1976

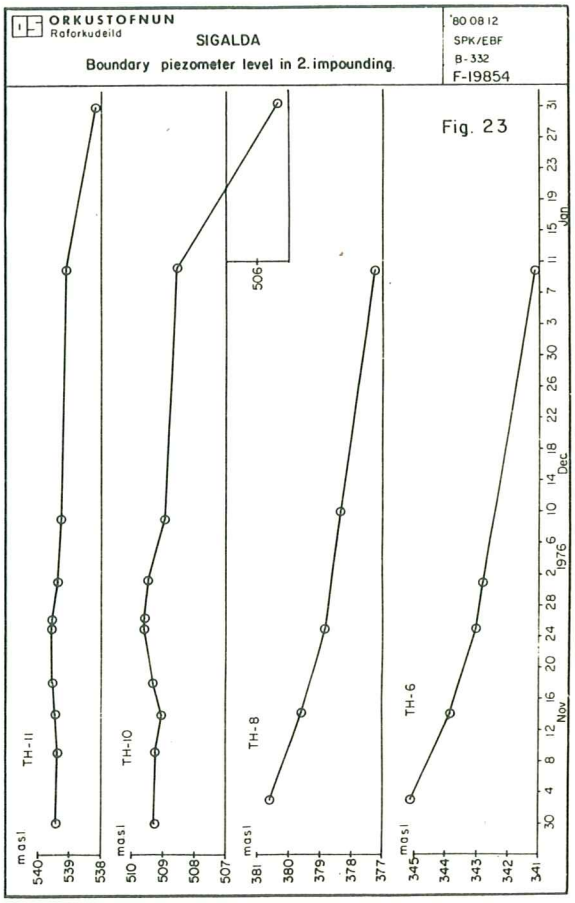
ORKUSTOFNUN
Raforkudeild
SIGALDA
Boundary piezometer level in 2. impounding.
'80 08 12
SPK/EBF
B-332
F-19854
Fig. 23
TH-11
TH-10
TH-8
TH-6
506
m a s l
Nov
Dec
1976
Jan

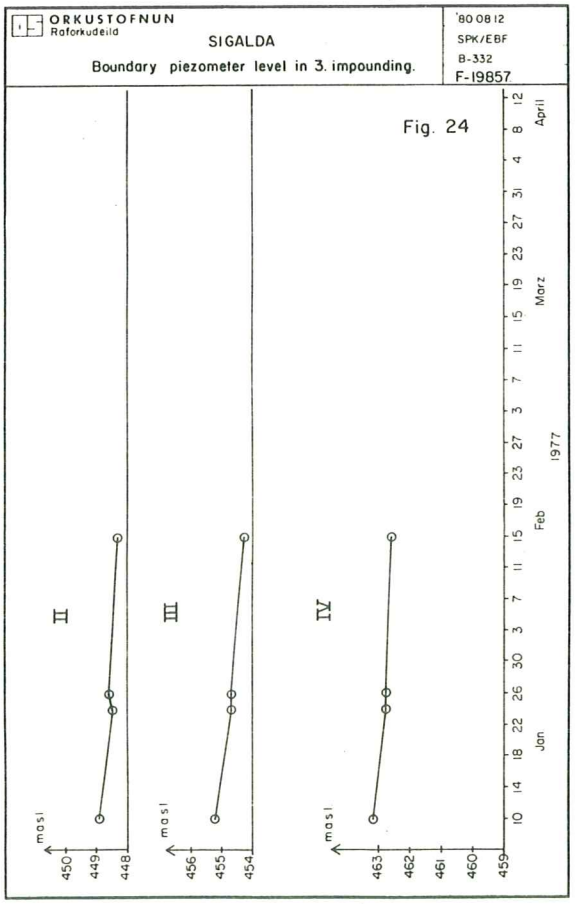
ORKUSTOFNUN
Raforkudeild
SIGALDA
Boundary piezometer level in 3. impounding.
'80 08 12
SPK/EBF
B-332
F-19857
Fig. 24
II
III
IV
m a s l
Jan
Feb
Marz
April
1977

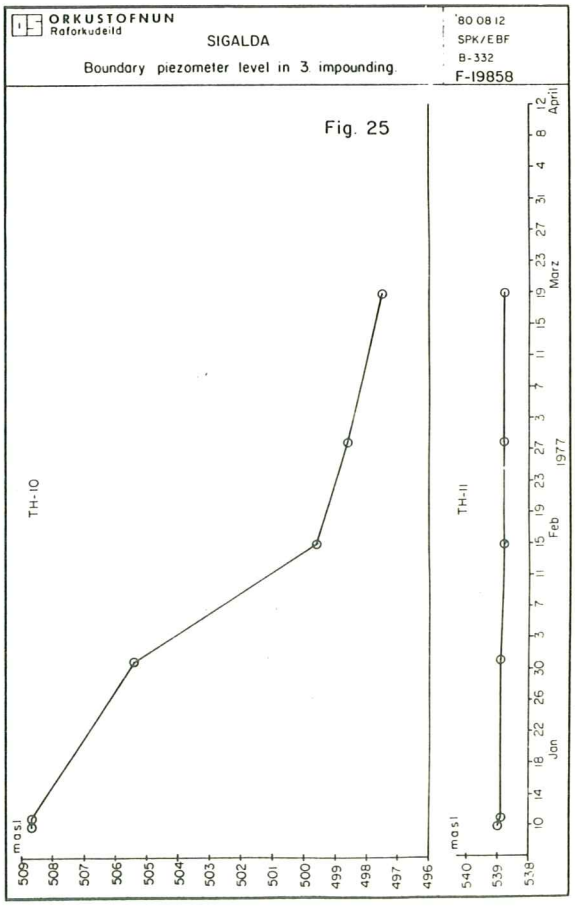
ORKUSTOFNUN
Raforkudeild
SIGALDA
Boundary piezometer level in 3. impounding.
'80 08 12
SPK/EBF
B-332
F-19858
Fig. 25
TH-10
TH-11
m a s l
Jan
Feb
Marz
April
1977

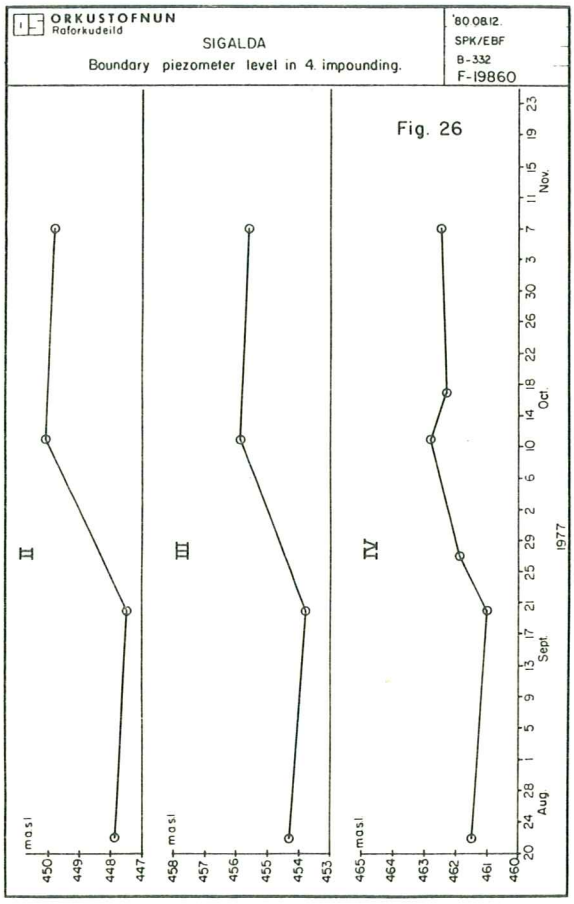
ORKUSTOFNUN
Raforkudeild
SIGALDA
Boundary piezometer level in 4. impounding.
'80.08.12.
SPK/EBF
B-332
F-19860
Fig. 26
II
III
IV
m.a.s.l.
Aug
Sept.
Oct.
Nov.
1977

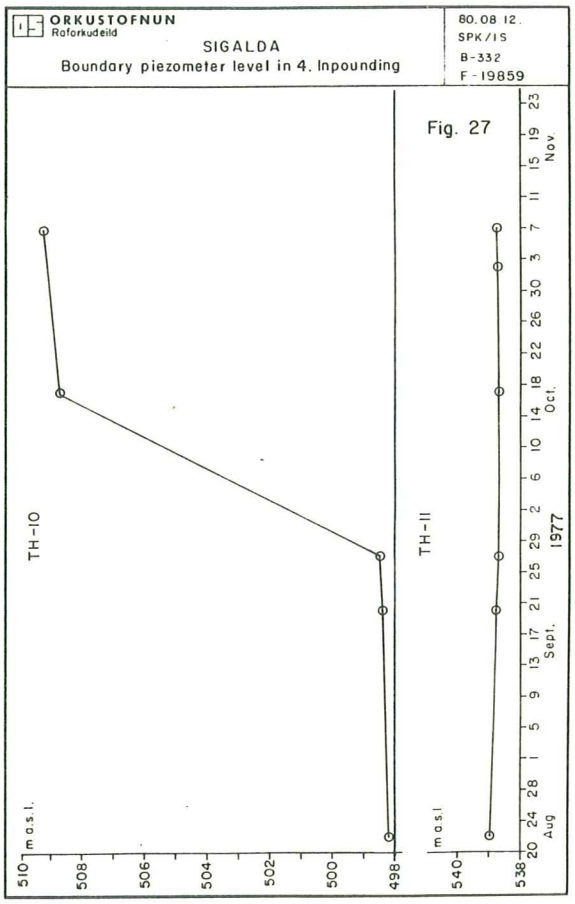
ORKUSTOFNUN
Raforkudeild
SIGALDA
Boundary piezometer level in 4. Inpounding
80.08.12.
SPK/IS
B-332
F-19859
Fig. 27
TH-10
TH-11
m.a.s.l.
Aug
Sept.
Oct.
Nov.
1977

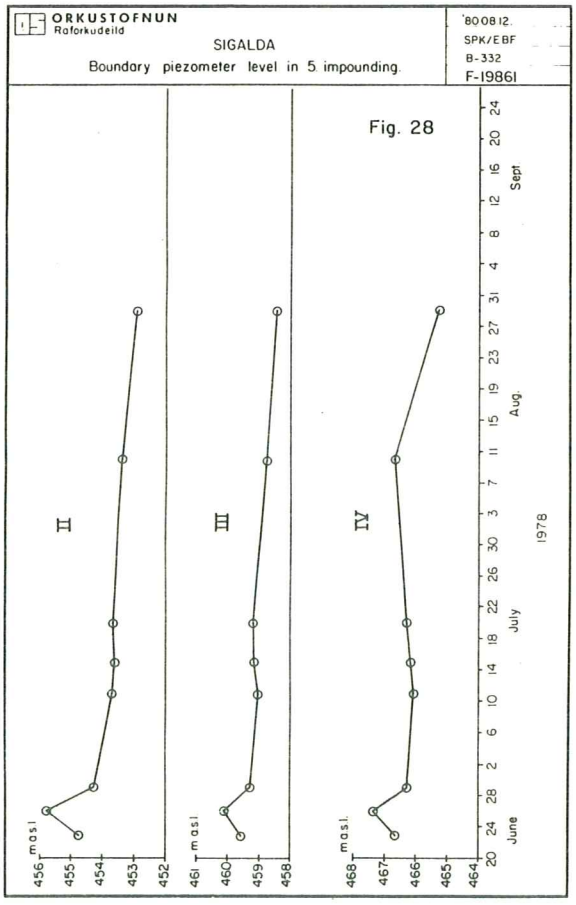
ORKUSTOFNUN
Raforkudeild
SIGALDA
Boundary piezometer level in 5. impounding.
'80.08.12.
SPK/EBF
B-332
F-19861
Fig. 28
II
III
IV
m.a.s.l.
June
July
Aug.
Sept
1978

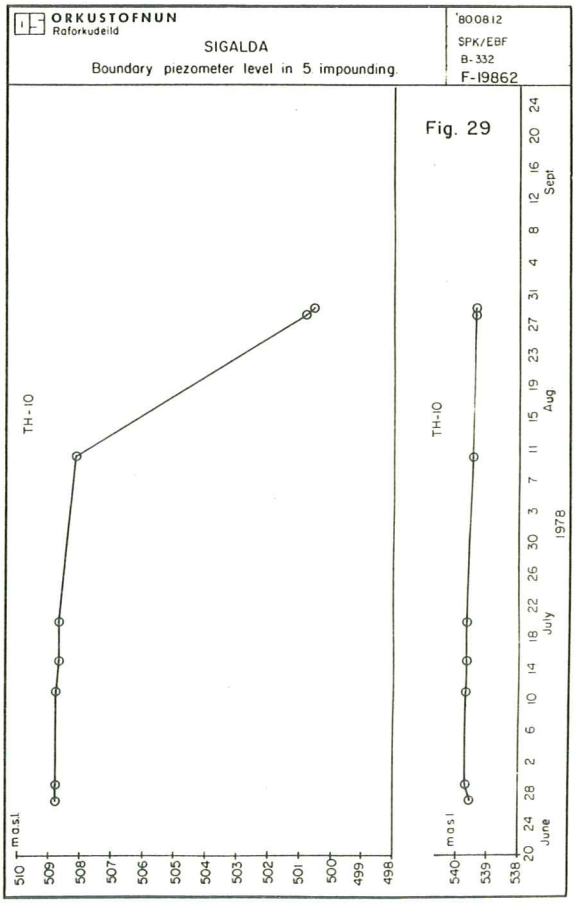
ORKUSTOFNUN
Raforkudeild
SIGALDA
Boundary piezometer level in 5. impounding.
'80.08.12
SPK/EBF
B-332
F-19862
Fig. 29
TH-10
TH-10
m.a.s.l.
June
July
Aug.
Sept
1978

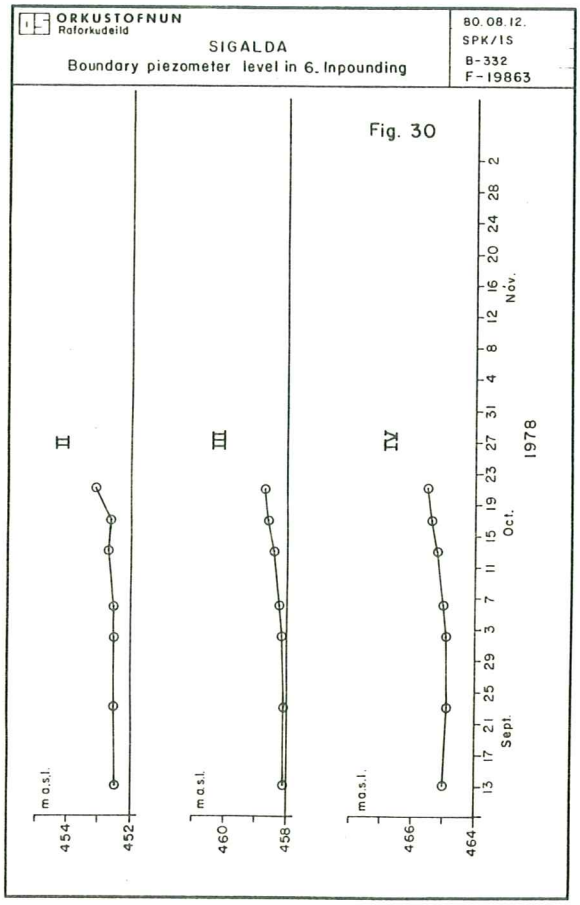
ORKUSTOFNUN
Raforkudeild
SIGALDA
Boundary piezometer level in 6. Inpounding
80.08.12.
SPK/IS
B-332
F-19863
Fig. 30
II
III
IV
m a.s.l.
Sept.
Oct.
Nov.
1978

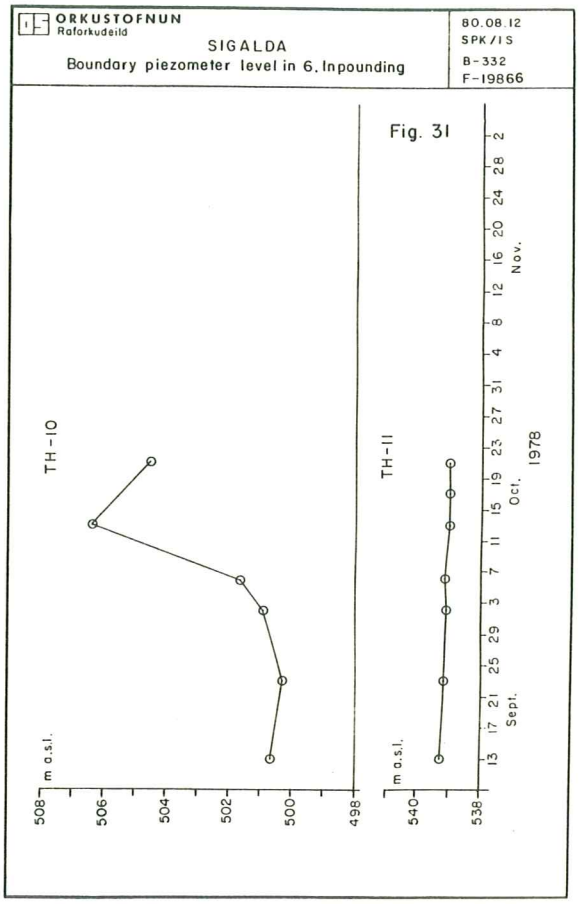
ORKUSTOFNUN
Raforkudeild
SIGALDA
Boundary piezometer level in 6. Inpounding
80.08.12
SPK/IS
B-332
F-19866
Fig. 31
TH-10
TH-11
m a.s.l.
Sept.
Oct.
Nov.
1978

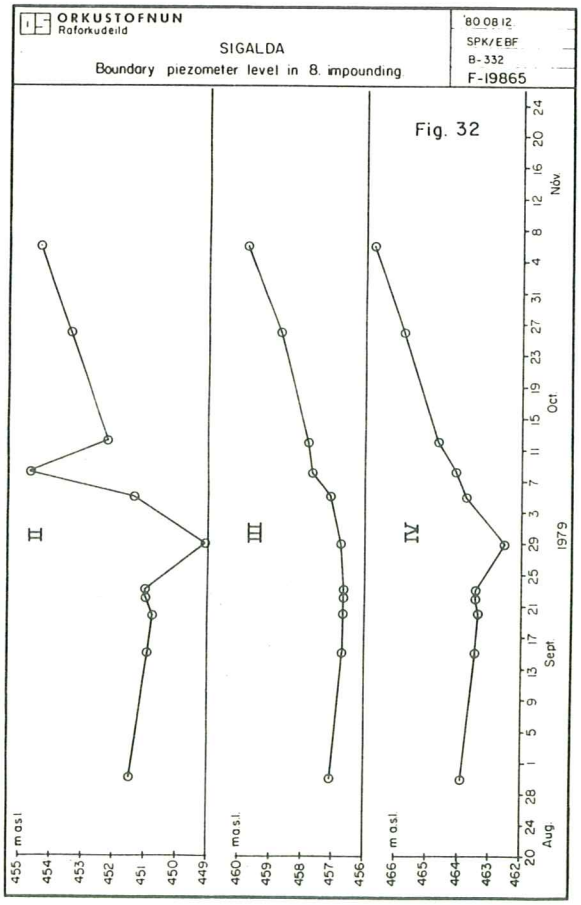
ORKUSTOFNUN
Raforkudeild
SIGALDA
Boundary piezometer level in 8. impounding
80.08.12
SPK/EBF
B-332
F-19865
Fig. 32
II
III
IV
m a.s.l.
Aug.
Sept.
Oct
Nov
1979

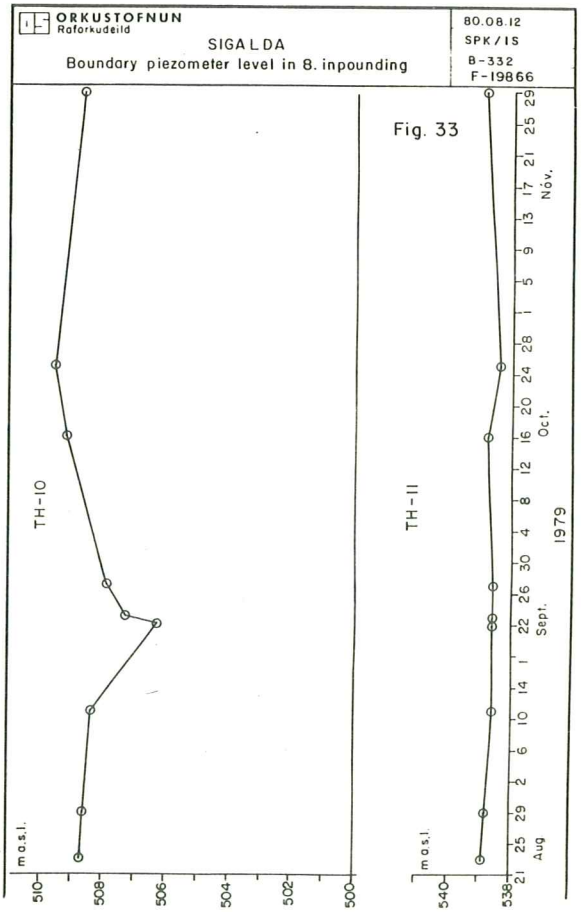
ORKUSTOFNUN
Raforkudeild
SIGALDA
Boundary piezometer level in 8. inpounding
80.08.12
SPK/IS
B-332
F-19866
Fig. 33
TH-10
TH-11
m a.s.l.
Aug.
Sept.
Oct.
Nov.
1979

ORKUSTOFNUN
Jarðhitadeild

SIGALDA
Linear flow component
Boundary flow parameter α vs. residual norm

80.07.29.
SPK / GSJ
B-332
F. 19833

Fig. 34

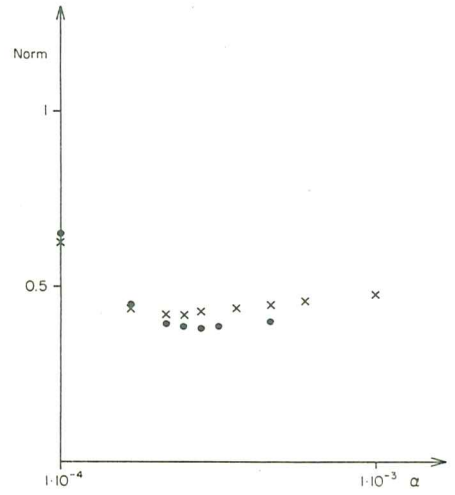

× Before sealing work

• After sealing work

ORKUSTOFNUN

SIGALDA
Linear flow component β
vs. residual norm

80.07.29.
SPK / GSJ
B-332
F. 19832

Fig. 35

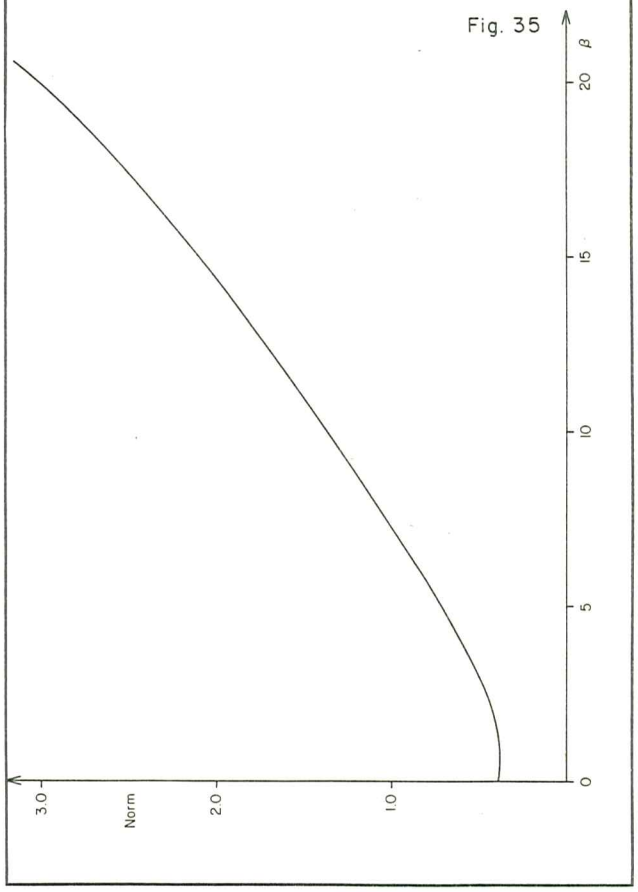

ORKUSTOFNUN

SIGALDA
Linear flow component β
vs. catchment loss / measured loss

80.07.29
SPK / GSJ
B-332
F. 19831

Fig. 36

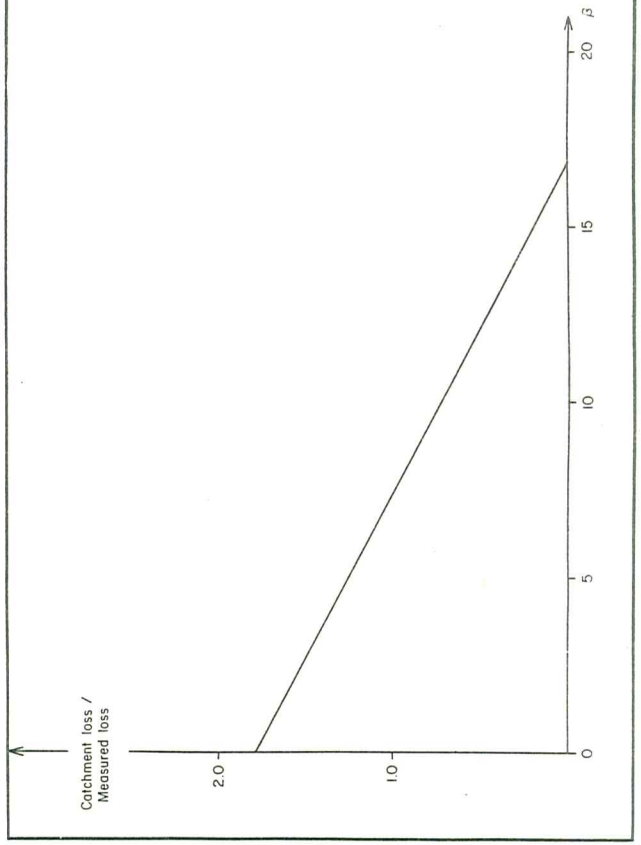

ORKUSTOFNUN
Jarðhitadeild

SIGALDA
Square flow component
Boundary flow parameter α vs. residual norm

80.07.29.
SPK / GSJ
B-332
F. 19834

Fig. 37

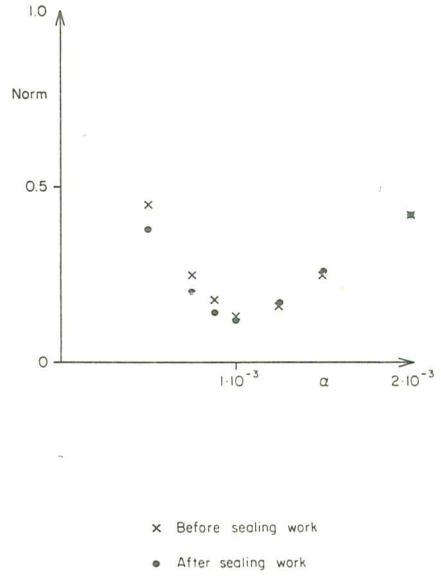

ORKUSTOFNUN

SIGALDA
Square flow component β
vs. residual norm

80.07.29.
SPK / GSJ
B-332
F. 19830

Fig. 38

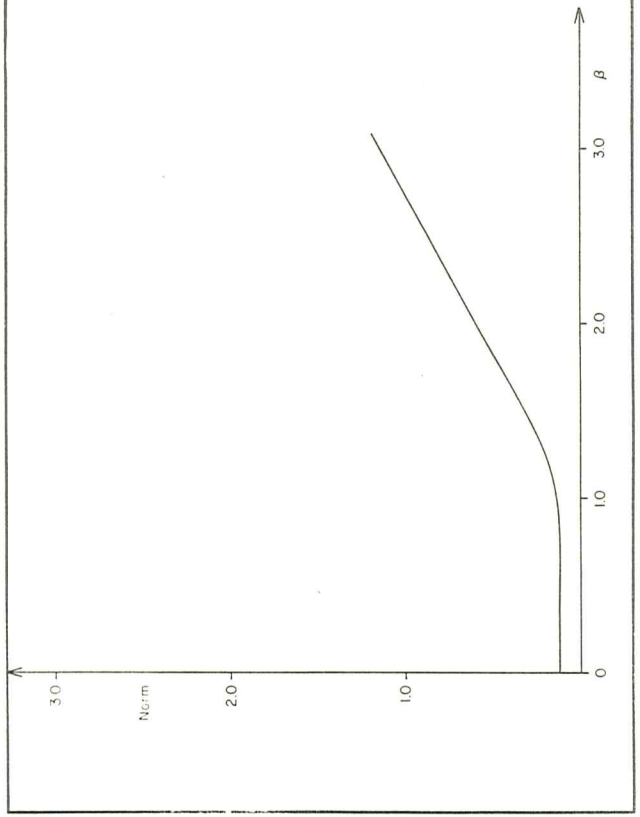

ORKUSTOFNUN
Jarðhitadeild

SIGALDA
Square flow component β vs.
Catchment loss / Measured loss

'80.09.01
SPK / ÓD
B-332
F. 19949

Fig. 39

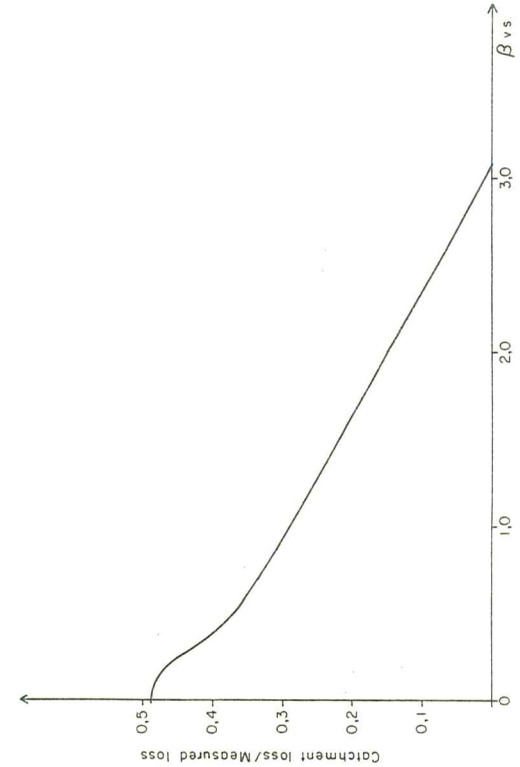

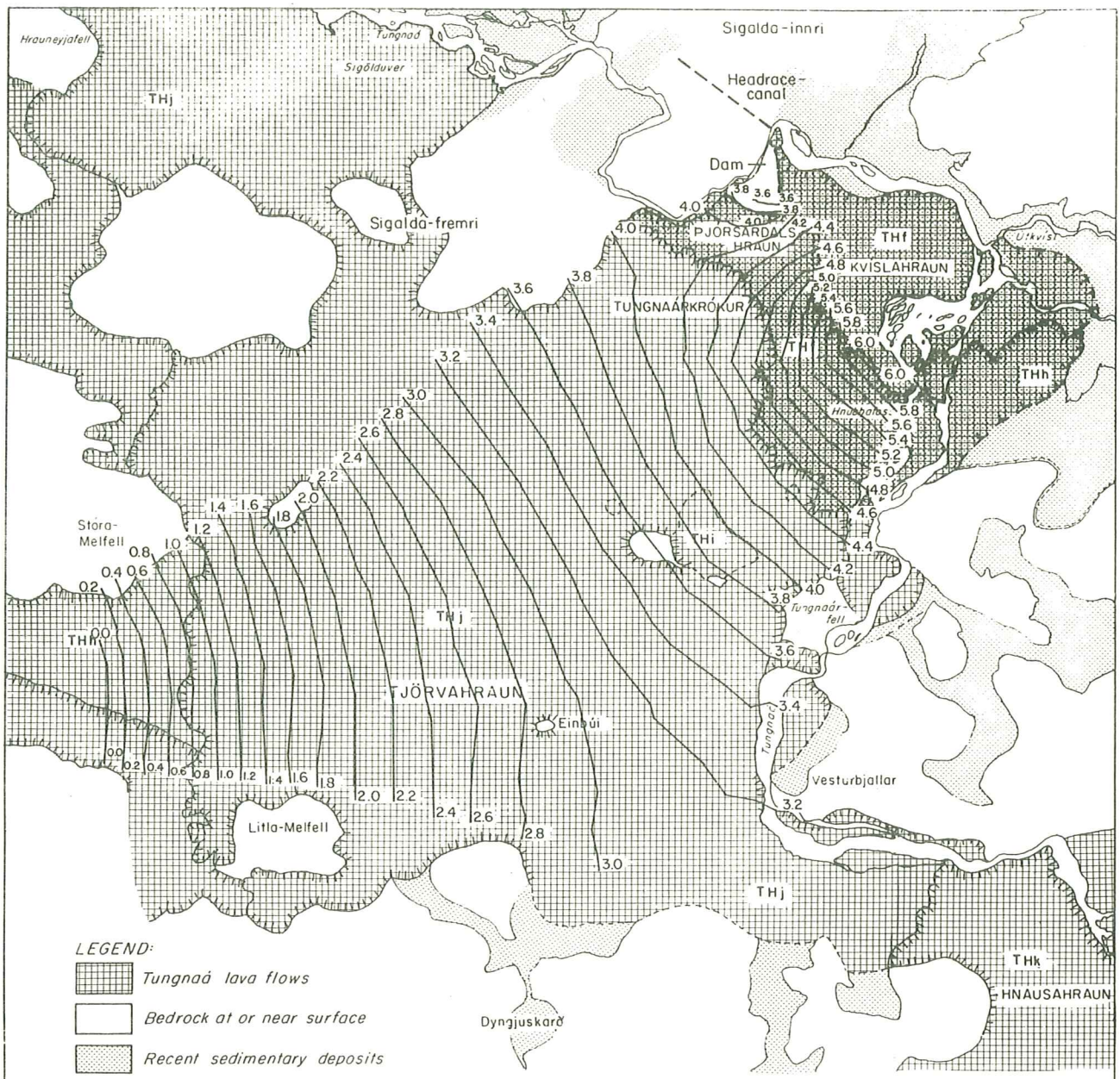

SIGALDA

Linear component before sealing work

Fig. 40

'80.09.01. SPK/ÓD B-332 F.19956

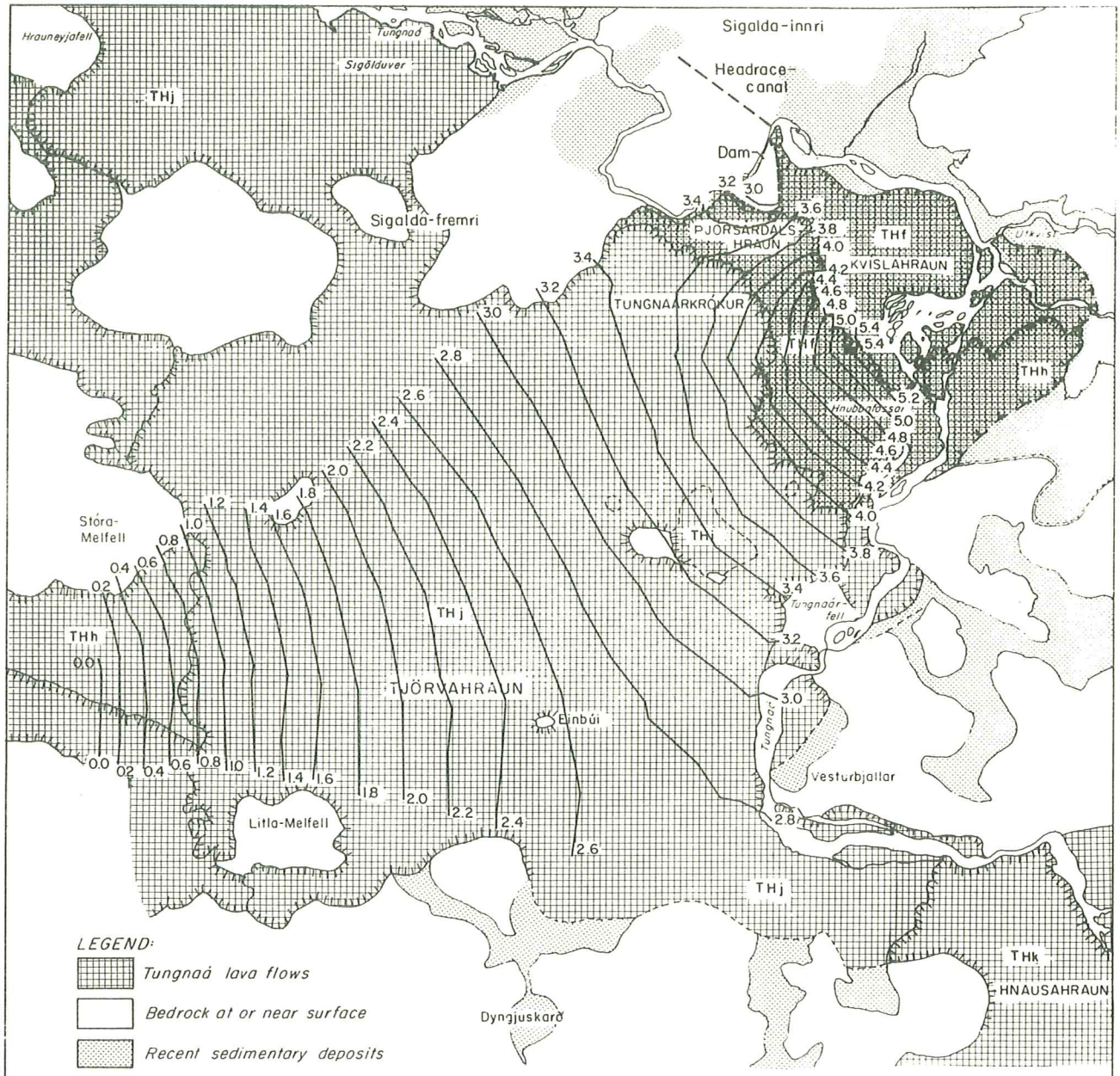

LEGEND:

- *Tungnaá lava flows*
- *Bedrock at or near surface*
- *Recent sedimentary deposits*
- *Sedimentary deposits on lava flows on Reservoir bottom*
- *Lavafronts*
- *Equivalue lines for linear component pr. 10m reservoir level rise from linear flow zero level*

SIGALDA

Linear component after sealing work

Fig. 41

'80.09.01. SPK/ÓD B-332

F. 19957

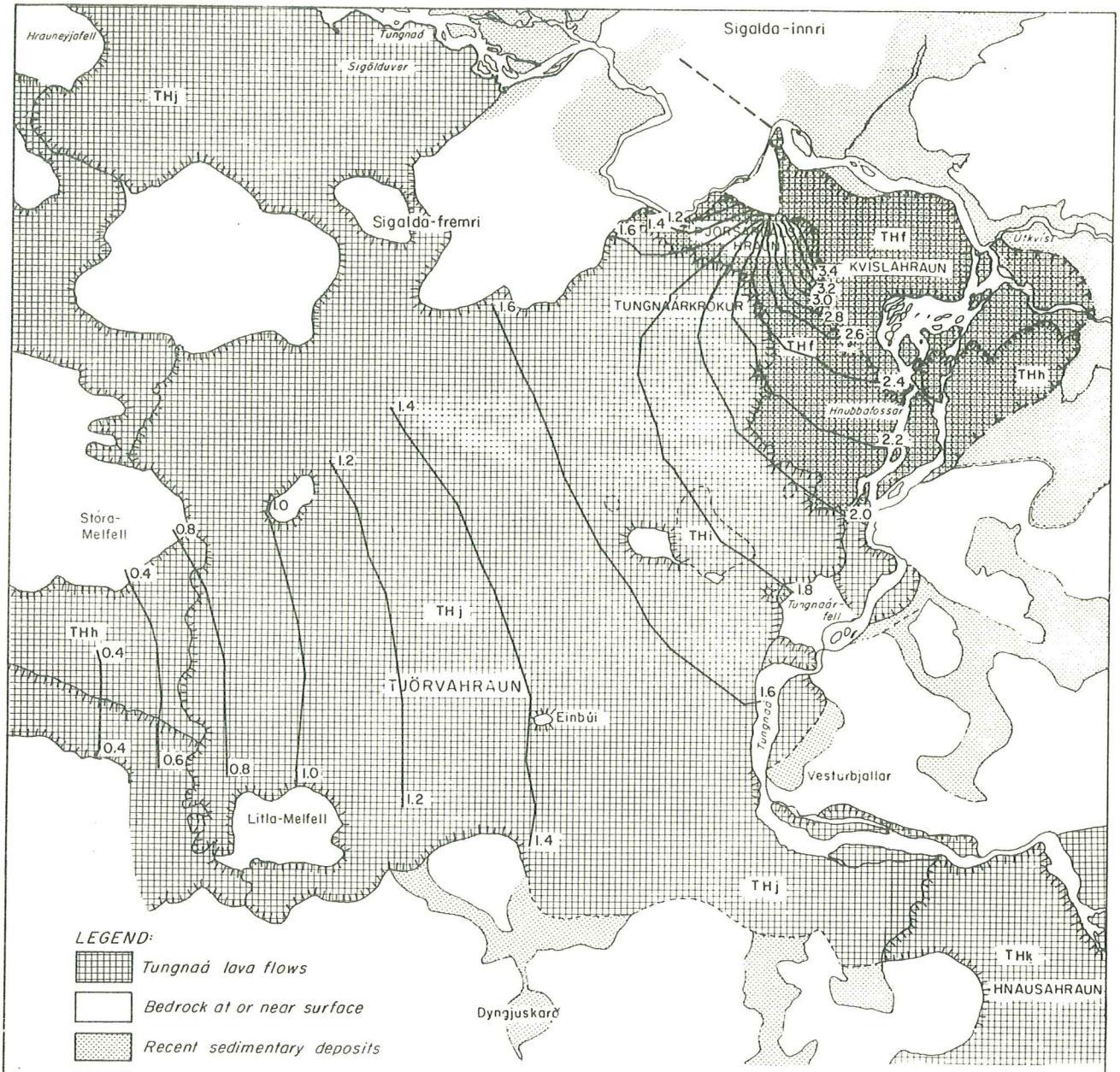

SIGALDA

Quadratic component before sealing work

Fig. 42

'80.09.01. SPK/ÓD B-332 F. 19953

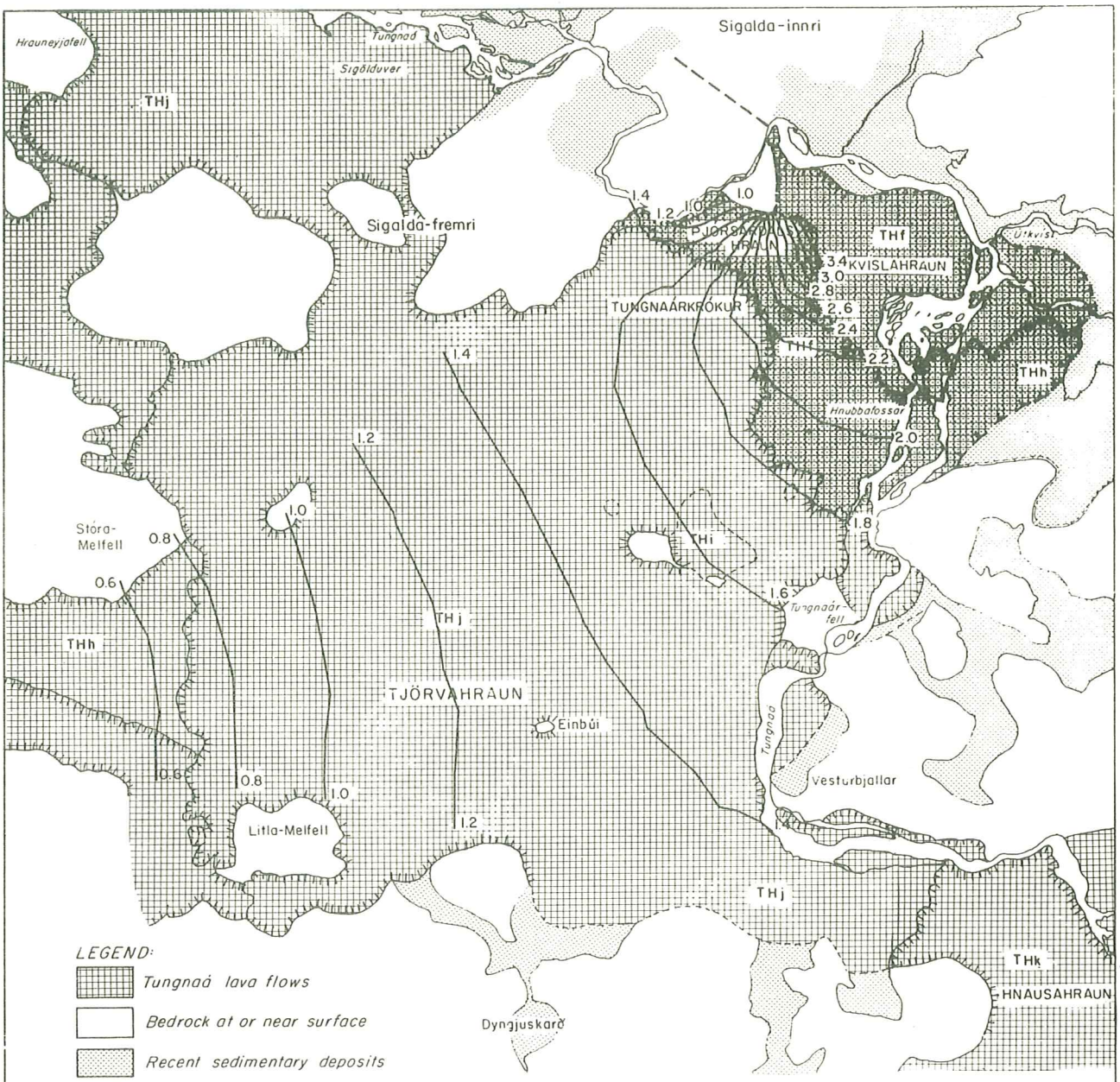

SIGALDA

Quadratic component after sealing work

Fig. 43

'80.09.01. SPK/ÓD B-332 F.19954

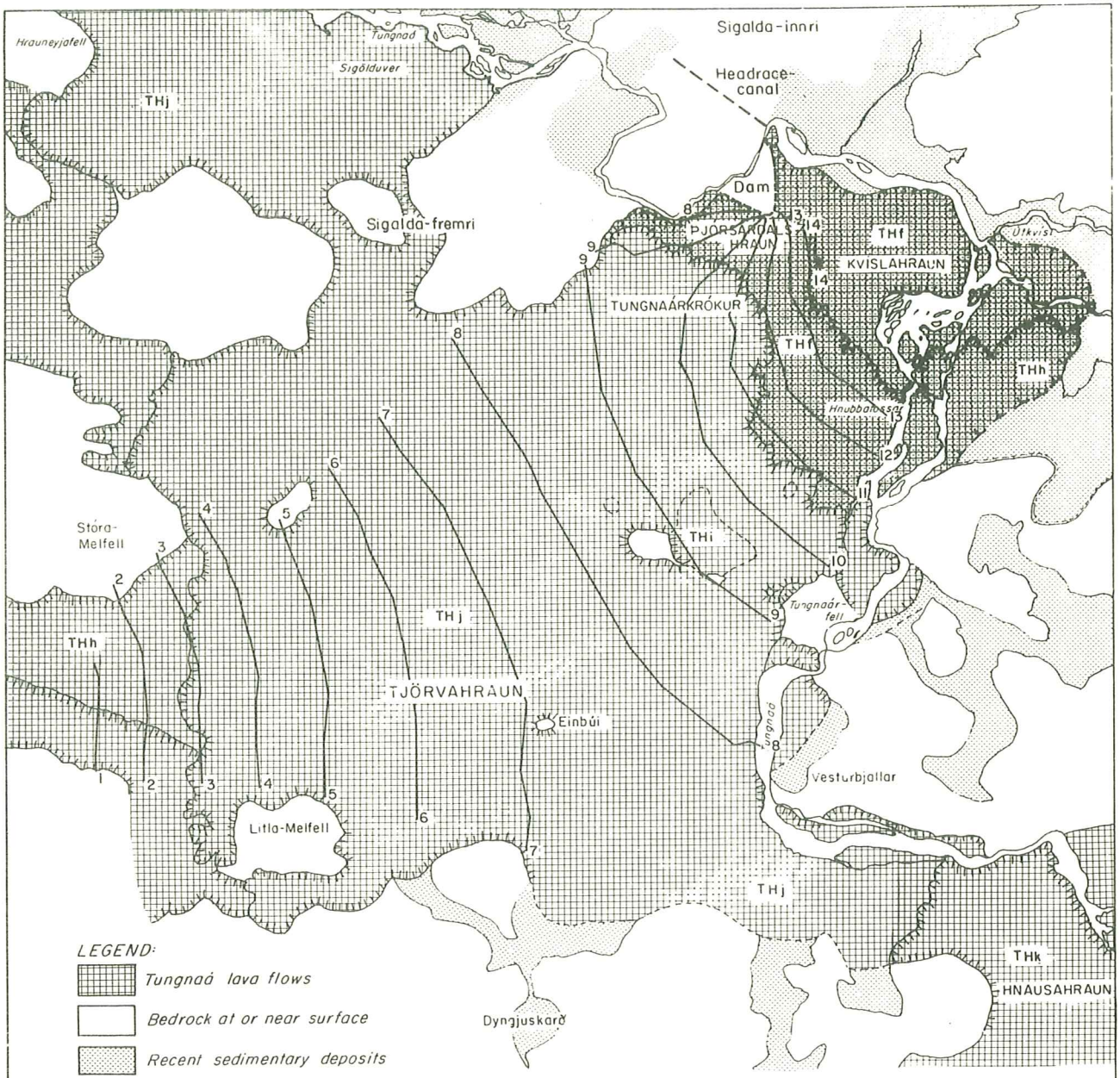

SIGALDA

Increase in piezometric level at reservoir level 493 m.a.s.l.

Fig. 44

'80.09.01. SPK/ÓD B-332 F. 19955

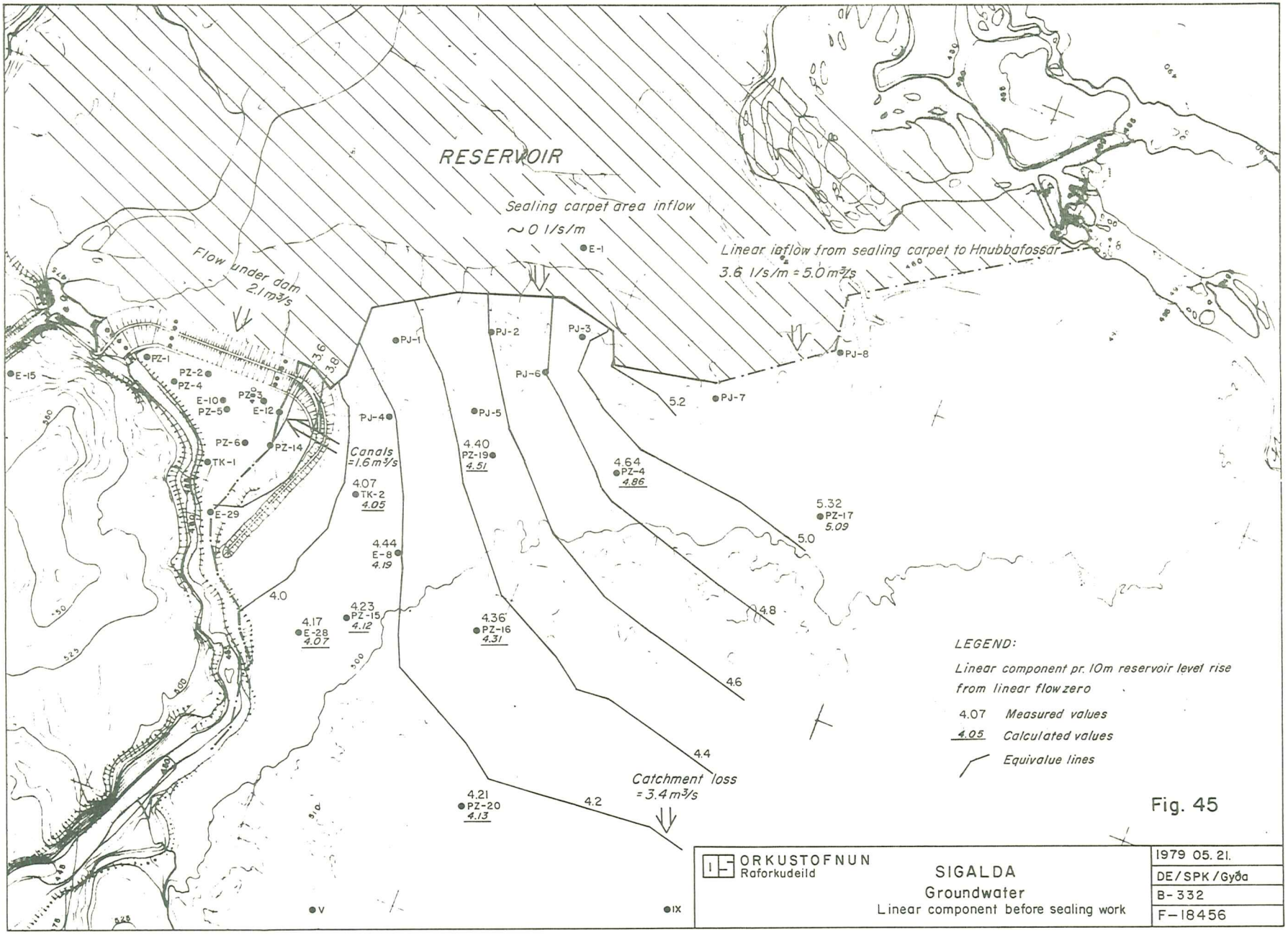
RESERVOIR
Sealing carpet area inflow
~0 l/s/m
Linear inflow from sealing carpet to Hnubbafossar
3.6 l/s/m = 5.0 m³/s
Flow under dam
2.1 m³/s
Canals
=1.6 m³/s
Catchment loss
=3.4 m³/s
E-1
E-15
PZ-1
PZ-2
PZ-4
E-10
PZ-5
PZ-3
E-12
PZ-6
PZ-14
TK-1
E-29
PJ-1
PJ-2
PJ-3
PJ-4
PJ-5
PJ-6
PJ-7
PJ-8
4.40
PZ-19
4.51
4.64
PZ-4
4.86
5.32
PZ-17
5.09
4.07
TK-2
4.05
4.44
E-8
4.19
4.17
E-28
4.07
4.23
PZ-15
4.12
4.36
PZ-16
4.31
4.21
PZ-20
4.13
5.2
5.0
4.8
4.6
4.4
4.2
4.0
3.8
3.6
V
IX
LEGEND:
Linear component pr. 10m reservoir level rise from linear flow zero
4.07 Measured values
4.05 Calculated values
Equivalue lines
Fig. 45
ORKUSTOFNUN
Raforkudeild
SIGALDA
Groundwater
Linear component before sealing work
1979 05. 21.
DE/SPK/Gyða
B-332
F-18456

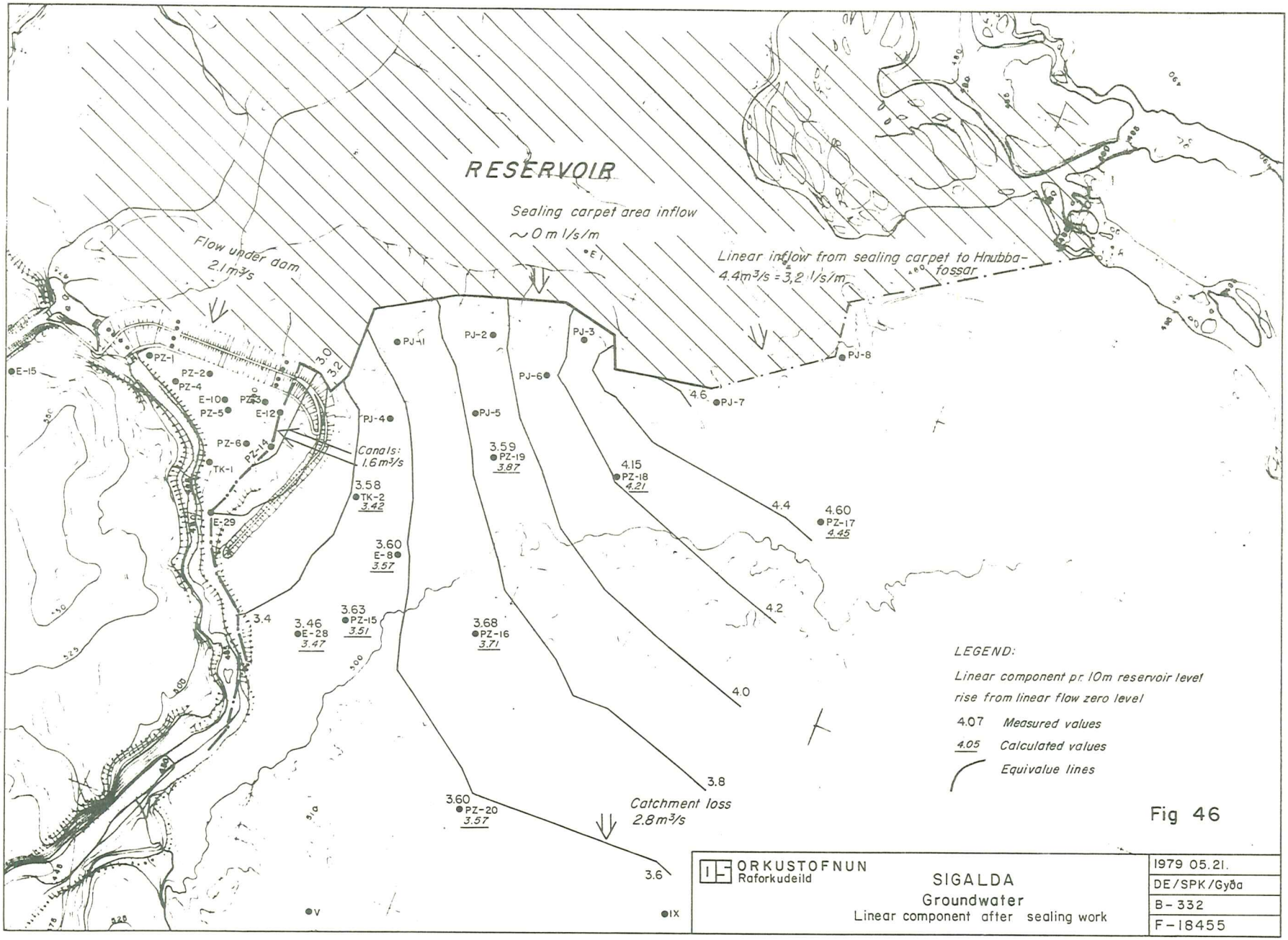
RESERVOIR
Sealing carpet area inflow
~0 m l/s/m
Flow under dam
2.1 m³/s
Linear inflow from sealing carpet to Hnubba-
4.4 m³/s = 3,2 l/s/m
fossar
Canals:
1.6 m³/s
Catchment loss
2.8 m³/s
PZ-1
PZ-2
PZ-4
E-10
PZ-3
PZ-5
E-12
PZ-6
PZ-14
TK-1
TK-2
3.42
E-29
E-15
E-1
PJ-1
PJ-2
PJ-3
PJ-4
PJ-5
PJ-6
PJ-7
PJ-8
3.59
PZ-19
3.87
4.15
PZ-18
4.21
4.60
PZ-17
4.45
3.60
E-8
3.57
3.63
PZ-15
3.51
3.46
E-28
3.47
3.68
PZ-16
3.71
3.60
PZ-20
3.57
3.0
3.2
3.4
4.6
4.4
4.2
4.0
3.8
3.6
LEGEND:
Linear component pr. 10m reservoir level rise from linear flow zero level
4.07 Measured values
4.05 Calculated values
Equivalue lines
Fig 46
ORKUSTOFNUN
Raforkudeild
SIGALDA
Groundwater
Linear component after sealing work
1979 05.21.
DE/SPK/Gyða
B-332
F-18455

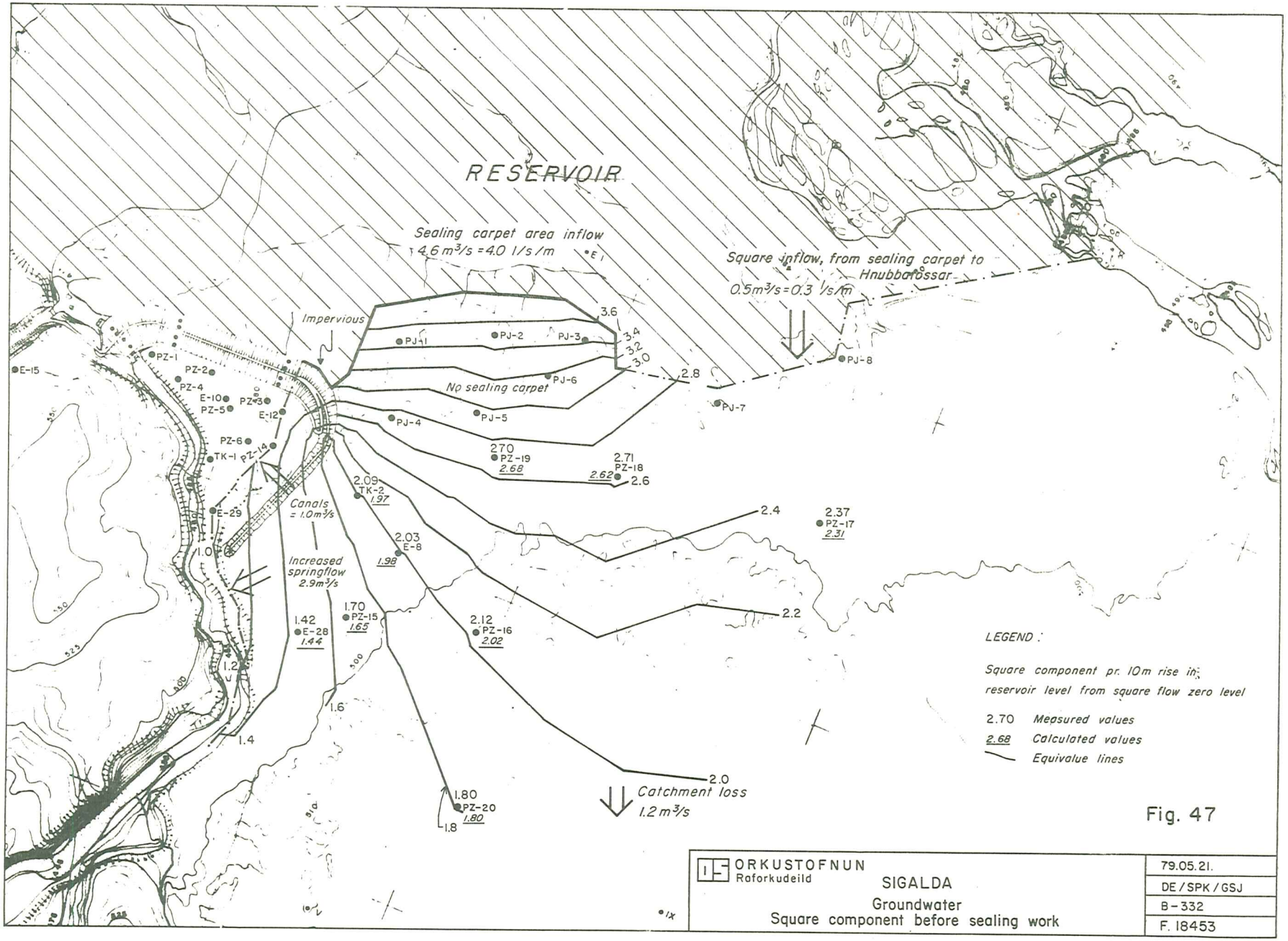

Fig. 47

ORKUSTOFNUN Raforkudeild	79.05.21.
SIGALDA	DE / SPK / GSJ
Groundwater	B - 332
Square component before sealing work	F. 18453

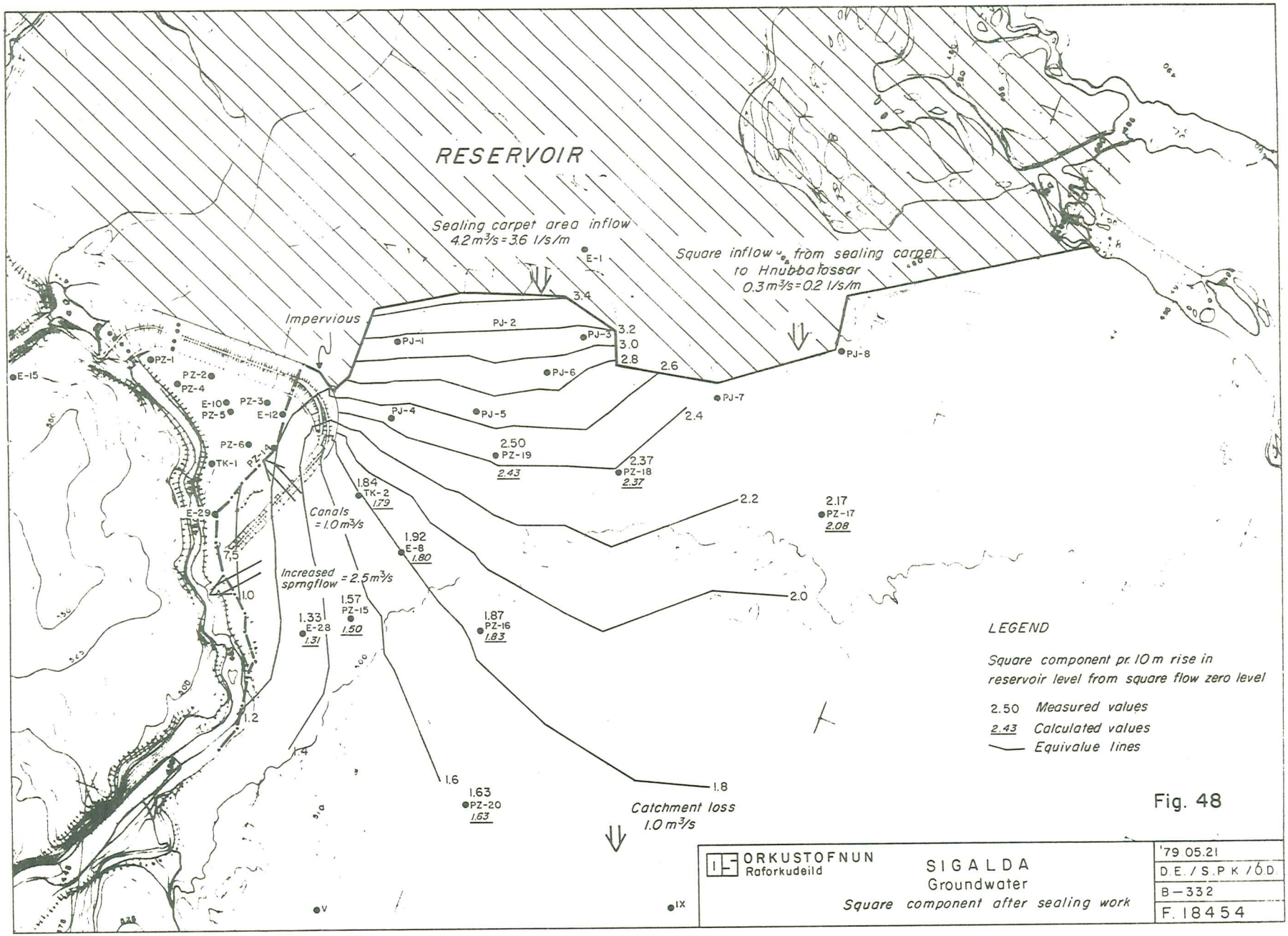
RESERVOIR
Sealing carpet area inflow
4.2 m³/s = 3.6 l/s/m
Square inflow from sealing carpet to Hnúbbafossar
0.3 m³/s = 0.2 l/s/m
Impervious
E-1
PJ-1
PJ-2
PJ-3
PJ-4
PJ-5
PJ-6
PJ-7
PJ-8
3.4
3.2
3.0
2.8
2.6
2.4
2.2
2.0
PZ-1
PZ-2
PZ-3
PZ-4
PZ-5
PZ-6
E-10
E-12
E-15
TK-1
2.50
PZ-19
2.43
2.37
PZ-18
2.37
2.17
PZ-17
2.08
1.84
TK-2
1.79
1.92
E-8
1.80
1.87
PZ-16
1.83
1.57
PZ-15
1.50
1.33
E-28
1.31
1.63
PZ-20
1.63
Canals
= 1.0 m³/s
Increased springflow = 2.5 m³/s
Catchment loss
1.0 m³/s
LEGEND
Square component pr. 10 m rise in reservoir level from square flow zero level
2.50 Measured values
2.43 Calculated values
Equivalue lines
Fig. 48
ORKUSTOFNUN
Raforkudeild
SIGALDA
Groundwater
Square component after sealing work
'79 05.21
D.E./S.P.K./G.D.
B-332
F. 18454

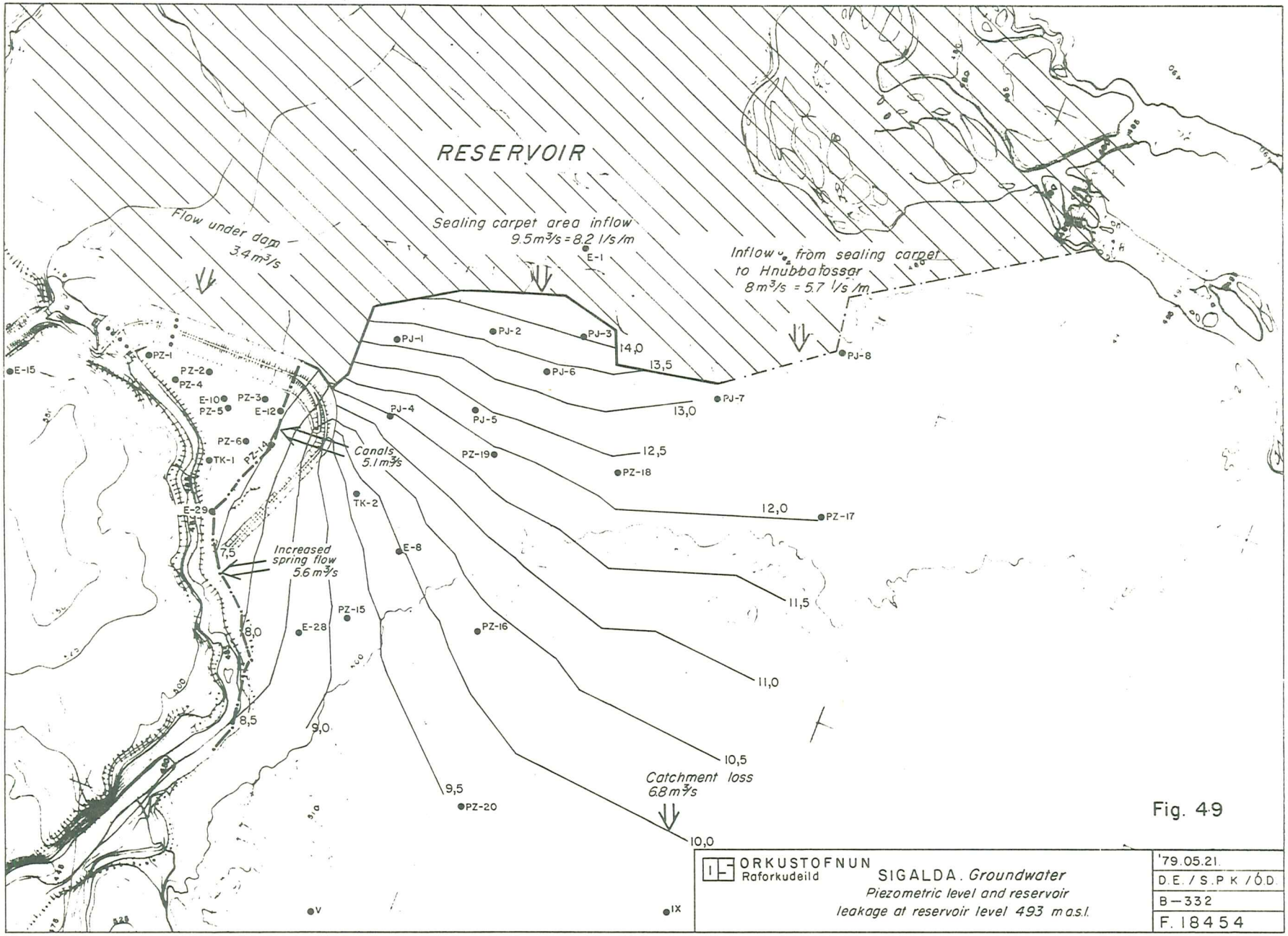

Fig. 4.9

ORKUSTOFNUN
Raforkudeild

SIGALDA. *Groundwater*
Piezometric level and reservoir leakage at reservoir level 493 m a.s.l.

'79.05.21.
D.E. / S.P K / ÓD.
B—332
F. 18454

ORKUSTOFNUN

SIGALDA

PJ-12 vs. Reservoir level

80.07.29.
SPK / GSJ
B-332
F. 19839

Fig. 50

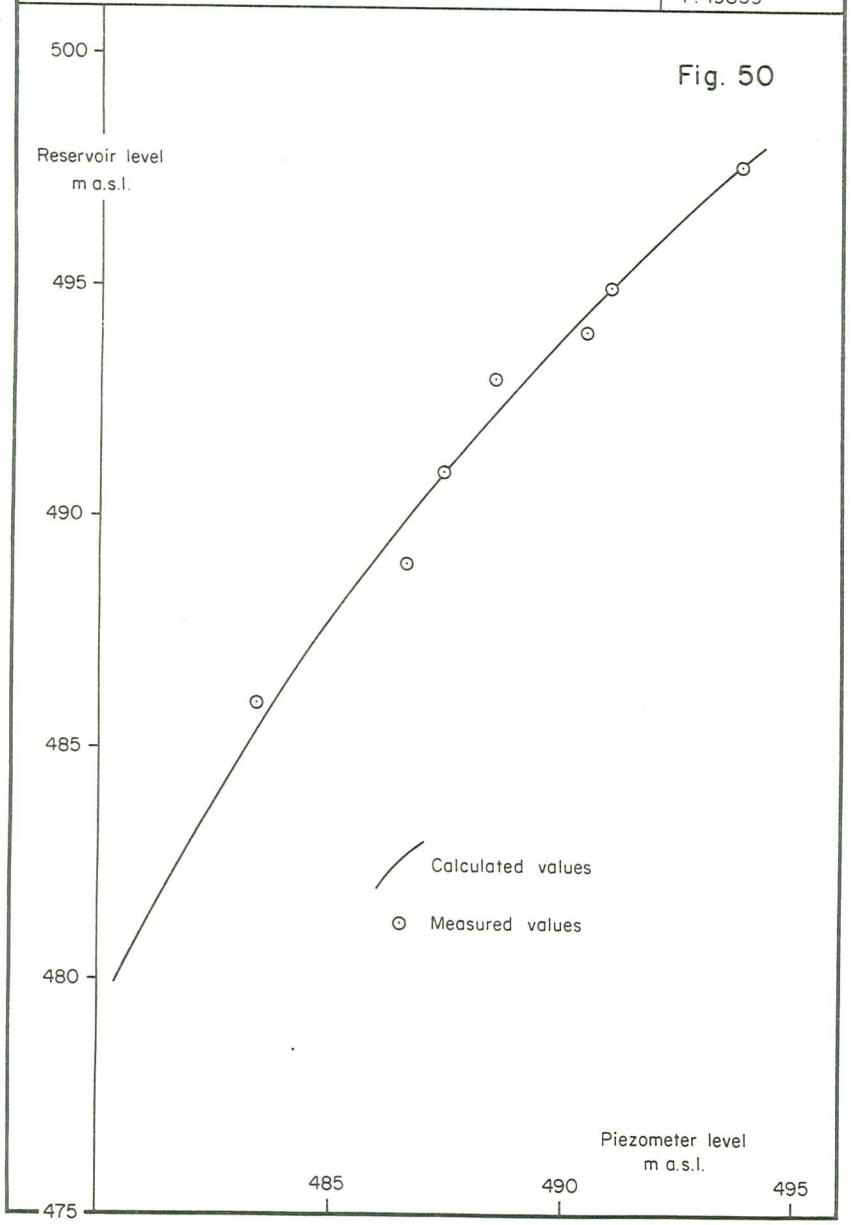

ORKUSTOFNUN

SIGALDA

VII vs. Reservoir level

80.07.29.
SPK / GSJ
B-332
F. 19841

Fig. 51

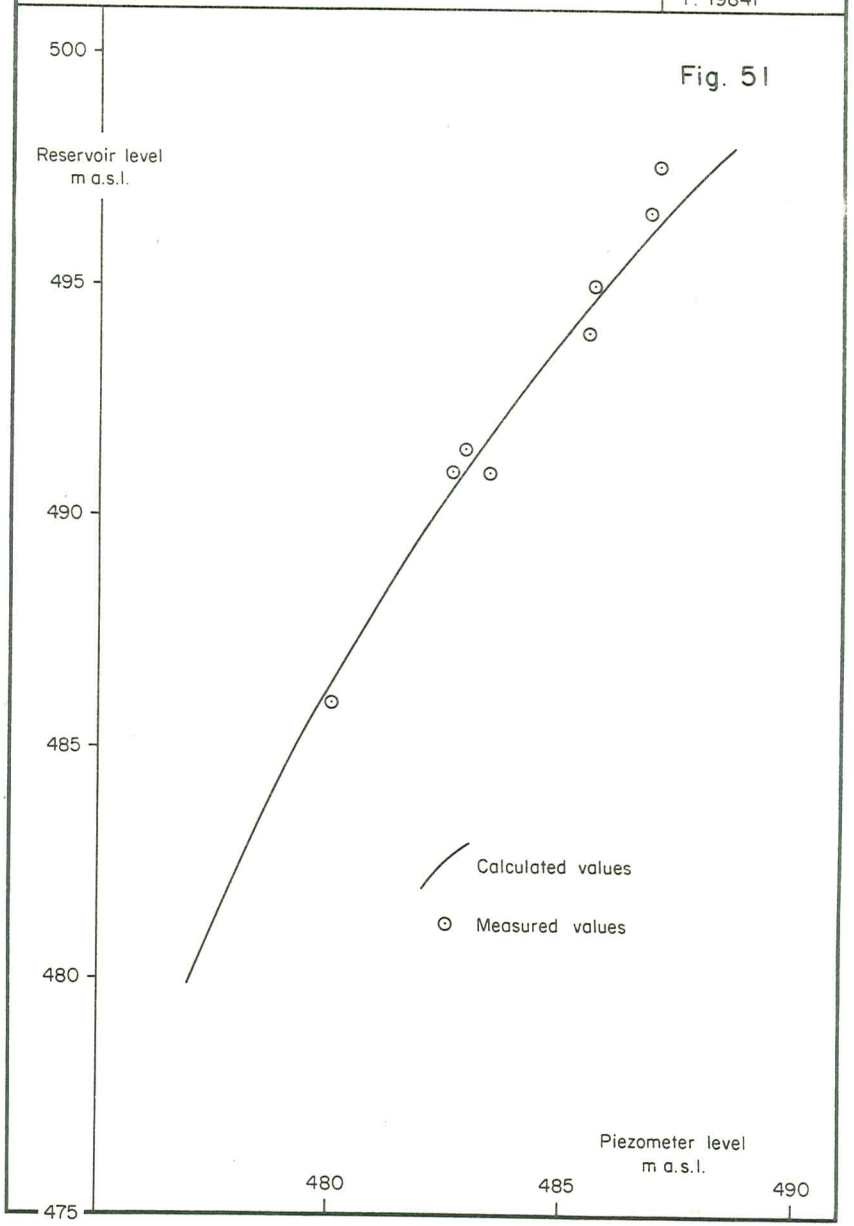

ORKUSTOFNUN

SIGALDA

VI vs. Reservoir level

80.07.40.
SPK / GSJ
B-332
F. 19840

Fig. 52

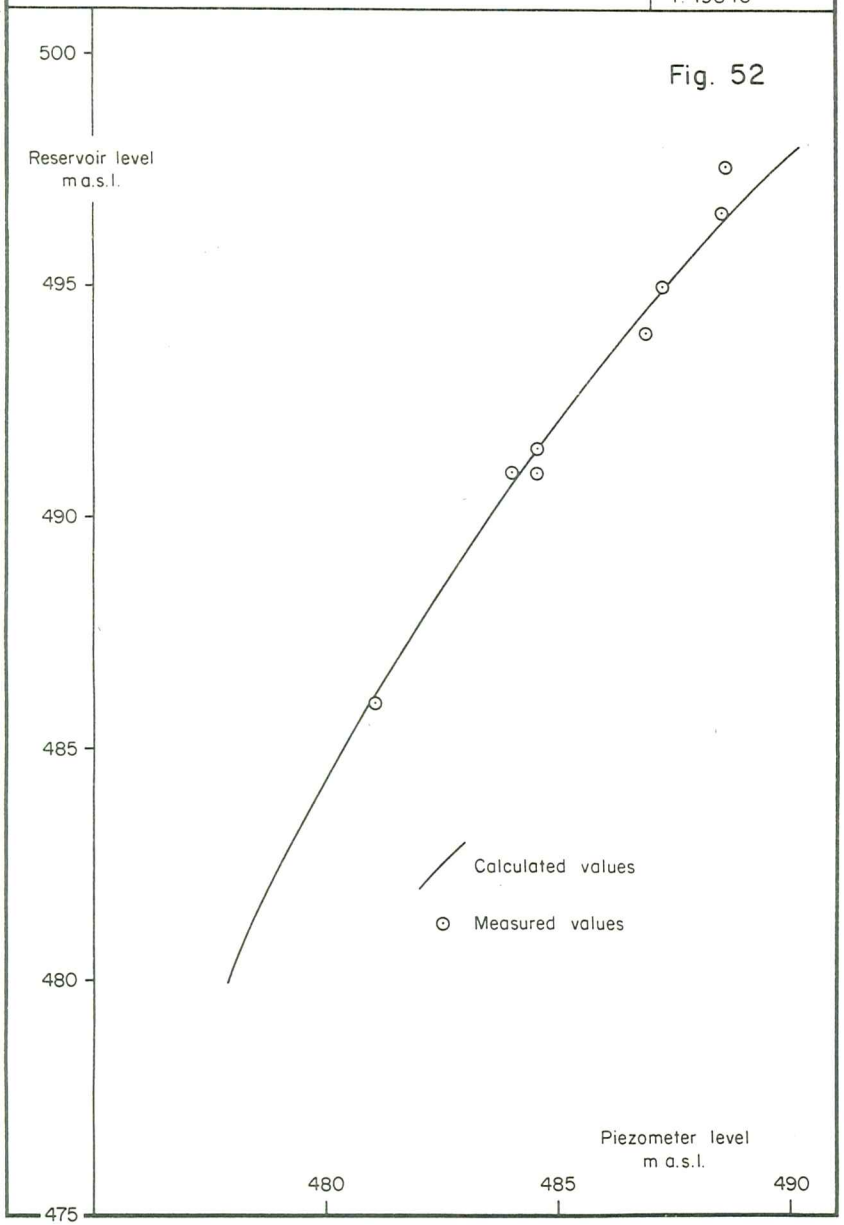

ORKUSTOFNUN

SIGALDA

PJ-11 vs. Reservoir level

80.07.29.
SPK / GSJ
B-332
F. 19838

Fig. 53

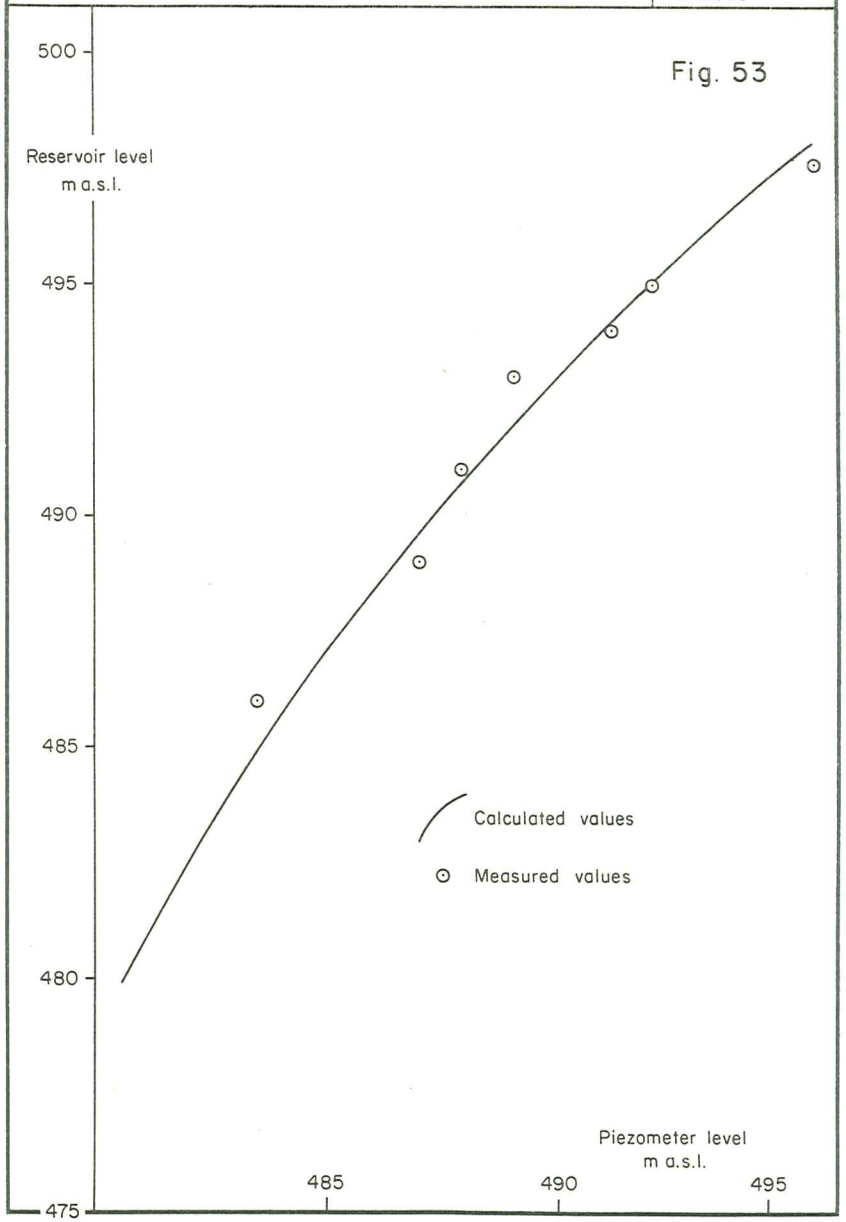

ORKUSTOFNUN

SIGALDA

TK-12 vs. Reservoir level

80.07.29.
SPK / GSJ
B-332
F. 19837

Fig. 54

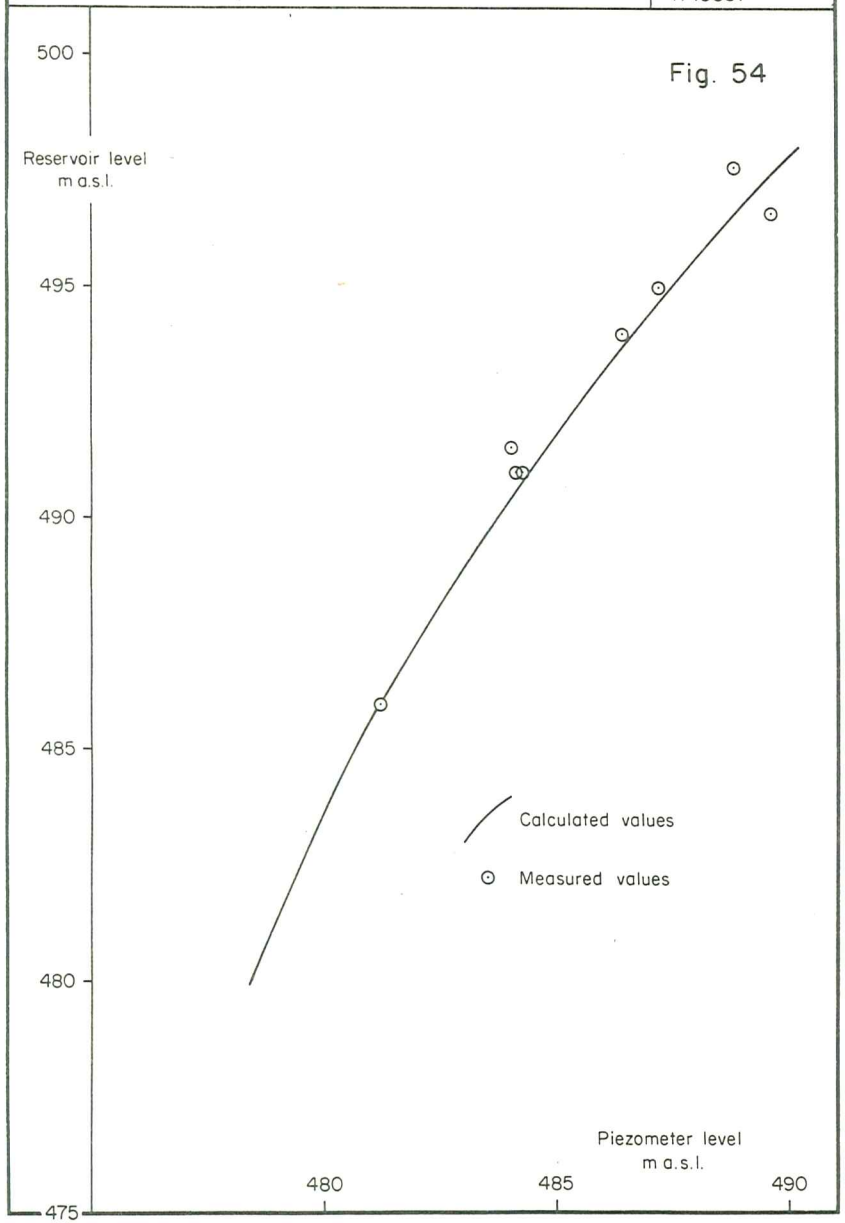

ORKUSTOFNUN

SIGALDA

V vs. Reservoir level

80.07.29.
SPK / GSJ
B-332
F. 19836

Fig. 55

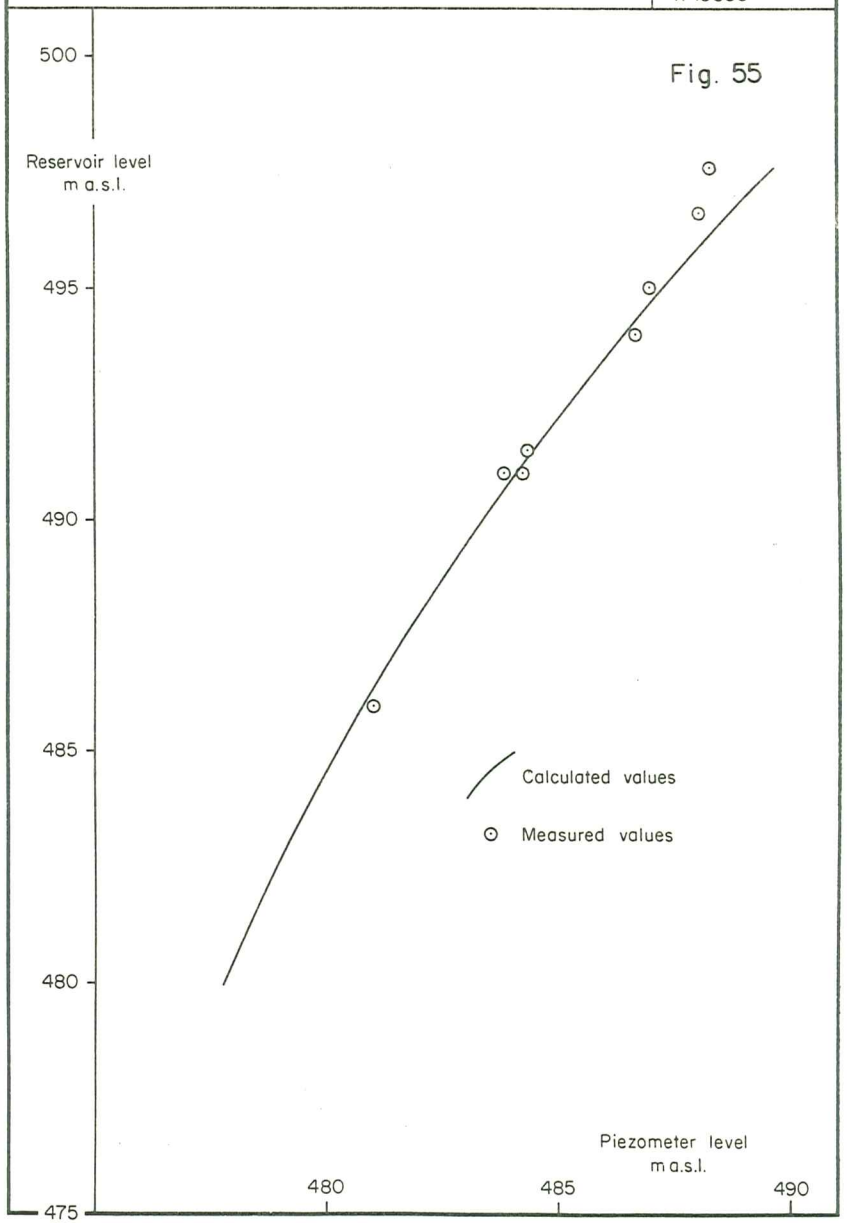

'80.09.01. SPK/ÓD
B-332
F. 19951

SIGALDA
IX vs. Reservoir level

Fig. 56

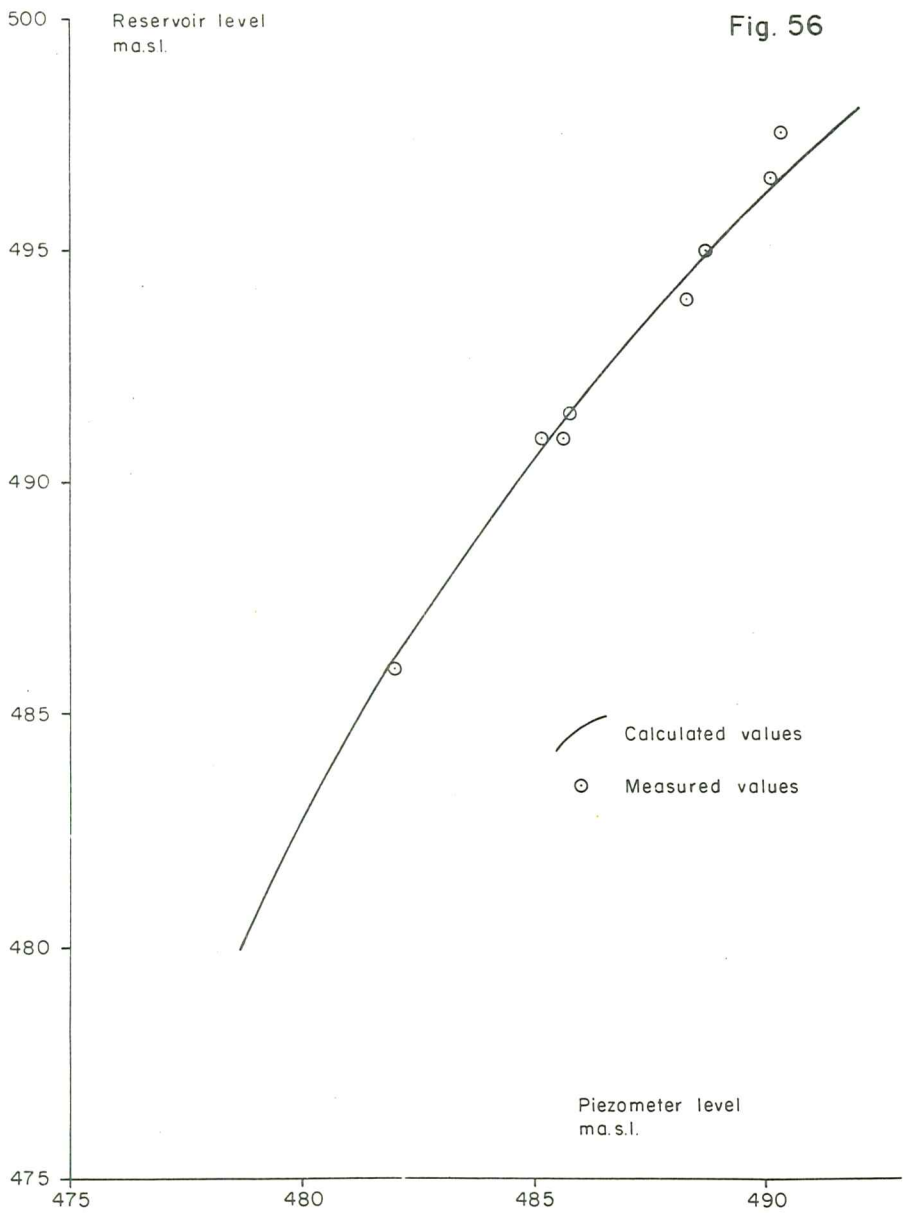

ORKUSTOFNUN
Jarðhitadeild

SIGALDA
Maximum effect of sealing carpet
vs. reservoir level

80.07.29.
SPK / GSJ
B-332
F. 19835

Fig. 57

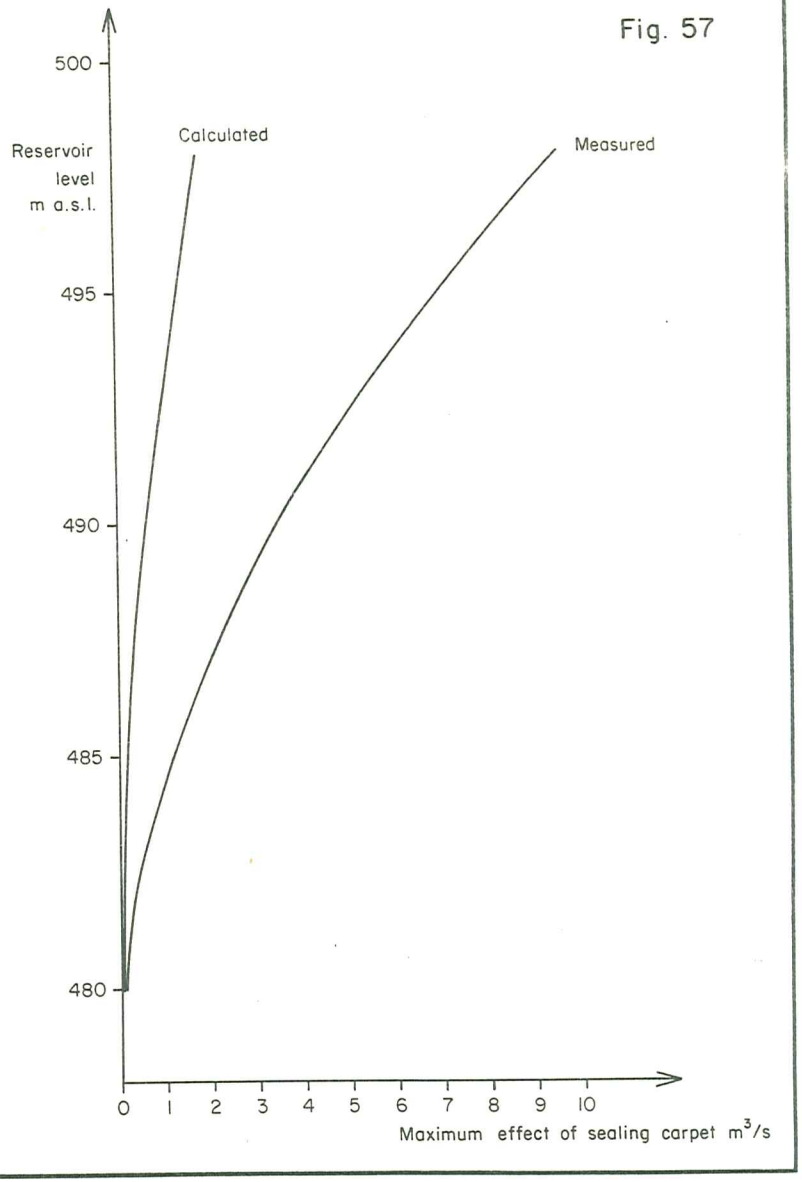

ORKUSTOFNUN

SIGALDA

Measured loss vs. reservoir level

80.07.27.
SPK / GSJ
B-332
F. 19827

Fig. 58

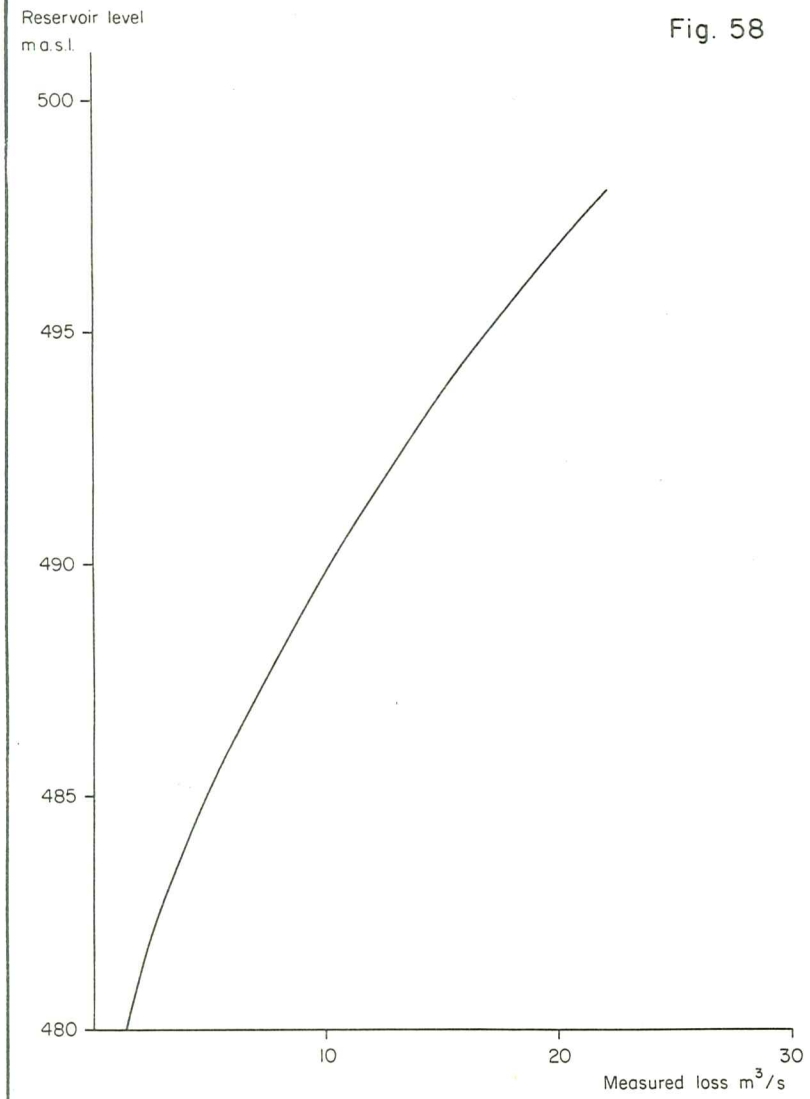

ORKUSTOFNUN

SIGALDA

Catchment loss vs. reservoir level

80.07.29.
SPK / GSJ
B-332
F. 19829

Fig. 59

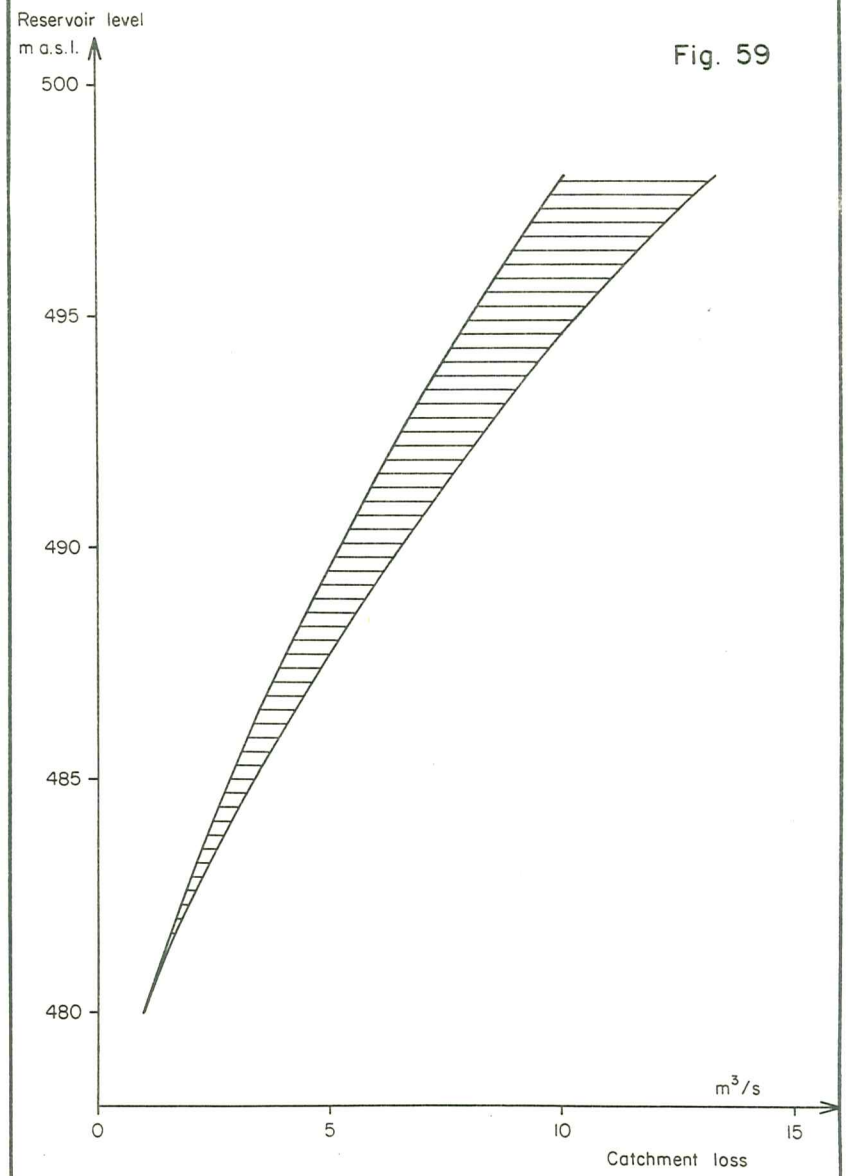

ORKUSTOFNUN

SIGALDA

Total loss vs. reservoir level

80.07.29.
SPK / GSJ
B-332
F. 19826

Fig. 60

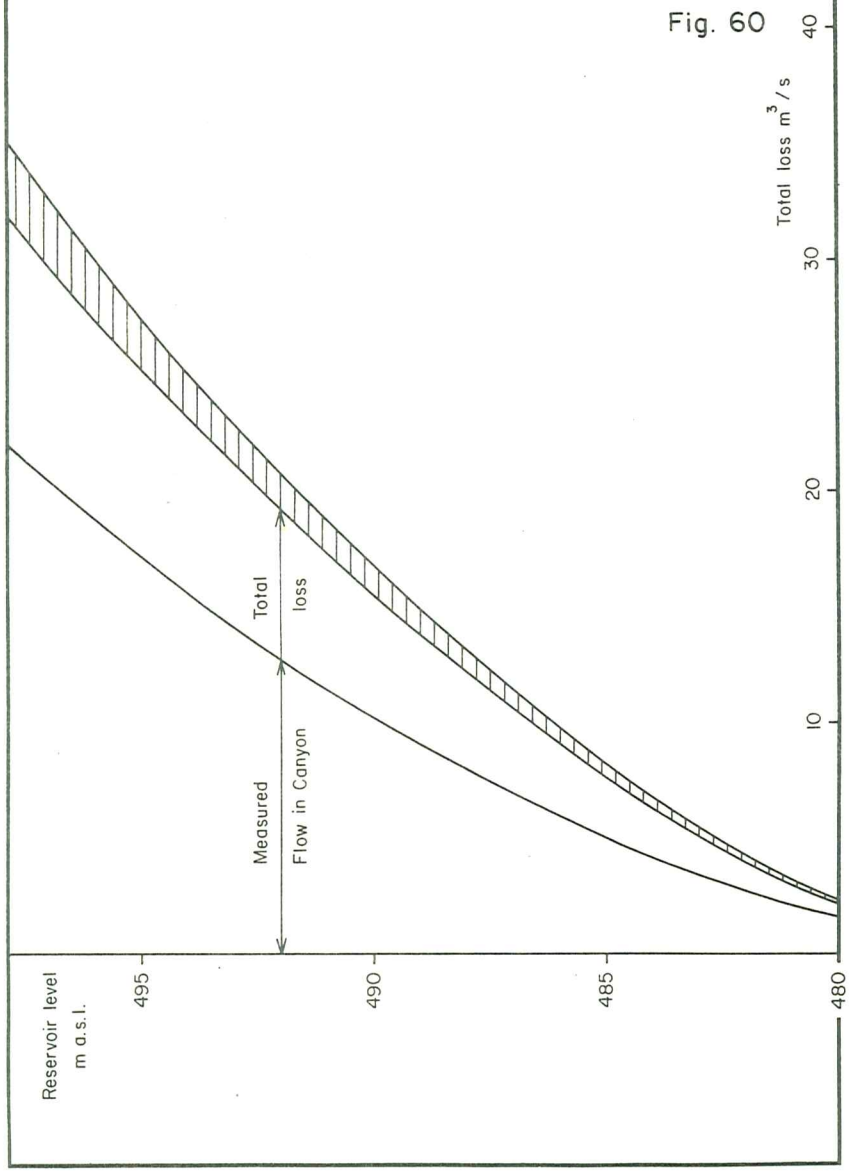

ORKUSTOFNUN

SIGALDA

Optimum energy reservoir level
vs. reservoir inflow

80.07.29.
SPK / GSJ
B-332
F. 19828

Fig. 61